# INVESTIGATION OF ATMOSPHERIC PHASE TRANSITIONS IN LOW TEMPERATURE, MIXED AEROSOLS

by

Aidan Neville Fredrick Bodsworth

A THESIS SUBMITTED IN PARTIAL FULFILLMENT OF THE REQUIREMENTS FOR THE DEGREE OF

MASTER OF SCIENCE

in

THE FACULTY OF GRADUATE STUDIES
(Chemistry)

The University of British Columbia
(Vancouver)

September 2010

# Abstract

Atmospheric aerosols are very small liquid or solid droplets which are suspended in a gas. They are present in our atmosphere in great numbers ($10^3$ particles per $cm^3$ in unpolluted rural environments). They represent a substantial source of uncertainty in climate models and influence human health, atmospheric reactivity and visibility. Field studies have shown that mixed organic-inorganic aerosols are abundant in the atmosphere. Mixed aerosols undergo phase transitions between aqueous and crystalline phases, called efflorescence and deliquescence. By examining laboratory prepared mixed droplets in a temperature and humidity controlled flow cell, these phase transitions were observed optically.

We studied the efflorescence properties of mixed citric acid-ammonium sulfate particles as a function of temperature to better understand the efflorescence properties of mixed organic-inorganic particles in the middle and upper troposphere. Data at 293 K illustrates that the addition of citric acid decreases the efflorescence relative humidity (ERH) of ammonium sulfate, which is consistent with the trends observed with other systems containing highly oxygenated organic compounds. At low temperatures the trend is qualitatively the same, but efflorescence can be inhibited by smaller concentrations of citric acid. For example at temperatures < 250 K an organic/(organic+sulfate) mass ratio of only 0.333 is needed to inhibit efflorescence of ammonium sulfate. In the upper troposphere the organic/(organic+sulfate) mass ratio can often be larger than this value.

We also studied phase transitions in ammonium sulfate-3-hydroxy-4-methoxy-mandelic acid (HMMA) systems. These systems showed similar trends in deliquescence and efflorescence to the citric acid case, but also underwent phase separations at an RH of approximately 77%. Again, low temperatures inhibited phase transitions.

It is believed that the inhibition of efflorescence and phase separation stems from either an increase in viscosity or the formation of an organic glass, this is investigated using classical nucleation theory and DSC measurements.

These studies imply that particles in the upper troposphere may be less likely to form or remain in the crystalline state than previously thought and that solid ammonium sulfate may be less likely to participate in heterogeneous ice nucleation in the upper troposphere. Additional studies are required on other model organic systems.

# Preface

Chapter 3 is a co-authored published article and chapter 4 represents collaborative work. The details of my contributions to each section are as follows:

Chapter 3 (First Authour status, accepted to PCCP, March 2010):

- Identified research program with help from supervisor.
- Modified existing apparatus from previous work to allow low temperature measurements.
- Calibrated and verified experimental set up.
- Performed all efflorescence and deliquescence data acquisition and analysis.
- Prepared all figures for the manuscript
- Shared manuscript preparation with my supervisor.
- DSC measurements taken by Dr. Zobrist at ETH, Zurich.

Chapter 4 (To be prepared for submission):

- Identified research program with help from supervisor.
- Calibrated and verified experimental set up.
- Performed all low temperature phase transition data acquisition (efflorescence, deliquescence and phase separation).
- Conducted all data analysis.
- Prepared all figures for the manuscript.
- Shared manuscript preparation with my supervisor.
- Additional room temperature measurements conducted by Chen Cen Aileen Liu.

# Table of Contents

# List of Tables

# List of Figures

## Acknowledgements

This thesis represents years of work and the efforts of many, many people who have helped me develop as a researcher and as an individual. I would thank the members of the Department of Chemistry at the University of British Columbia with whom I have enjoyed working. Dr. Allan Bertram, my supervisor, for providing so much support and the opportunity to begin research in atmospheric chemistry. I would also thank Dr. J. Scott Parent and Alf Kaethler, both of whom contributed and supported my love of chemistry with hours of help, attention to detail and support.

I have also learned countless invaluable things about research from the Bertram lab group, who taught me everything from the details of physical chemistry to turning on a hygrometer. Sarah, Emily, Jason, Michael, Donna, Song, Yuan, Simone, Pedro, Rich and Seb, you have been wonderful colleges and excellent friends, I'm proud to have learned chemistry from and with you all. Matt Parsons is another labmate who has contributed immensely to this project, I'd like to thank him for doing so much work developing the methodology and infrastructure which this project was built on. I'd also thank Chen Cen Aileen Liu for spending so much time running, researching and supporting this research.

I'm especially thankful to my family: Lois, Neville and Cameron. You have encouraged me when I was unmotivated and listened bemusedly as I struggled to explain what and why aerosols mattered. I've also been continually inspired by my Grandfather, Fred Bodsworth, who has always pushed me to be a better scientist, better environmentalist and better person.

I would also like to thank the UBC Hapkido club, especially Mike, Seb and Sorcha. You have provided me with constant support, feedback and energy from the very beginning of this degree. From everyone we trained with I've learned so much about pushing harder, trying more and achieving goals which I thought were impossible.

Finally, thanks to everyone who has supported me over the years. This extends to my friends, my climbing partners and my mentors, I'll can't list you all here but know that you've been important to me and I'll thank you in person.

# Dedication

To My Grandfather, Fred Bodsworth

# 1 Atmospheric Aerosols and their Properties

## 1.1 Atmospheric aerosols and their properties

Aerosols are suspensions of solids, liquids or mixtures of the two within a gas. Within the body of atmospheric literature, the term 'aerosol' is often used to describe just the particles, rather than the full suspension. Atmospheric aerosols are ubiquitous throughout the atmosphere with number concentrations from $10^3$ particles/cm$^3$ in rural regions to as high as $10^8$ particles/cm$^3$ in highly polluted urban environments[1]. These aerosols cover a wide size range, from <10 nm to ~100 μm, which is divided into two broad categories; coarse particles (>2.5 μm) and fine particles (<2.5 μm). In general coarse and fine modes have both different compositions and lifetimes. The distinction between different categories of aerosols is further examined in Figure 1.1, which shows several different modes based observed distributions during field studies.

Figure 1.1 shows measurements of atmospheric particles according to three different parameters; absolute number, surface area and volume. Analysis according to these varied parameters shows that no individual measurement provides a complete picture of aerosol size distribution. The absolute number measurements provide an excellent measure of very fine particles, but fail to account for a relatively small number of larger particles. Similarly, measurements of volume are biased to recognize the most massive particles. Thus, by measuring a variety of parameters a complete picture of aerosol's size distribution can be developed. The different modes stem from a wide the variety of sources and sinks.

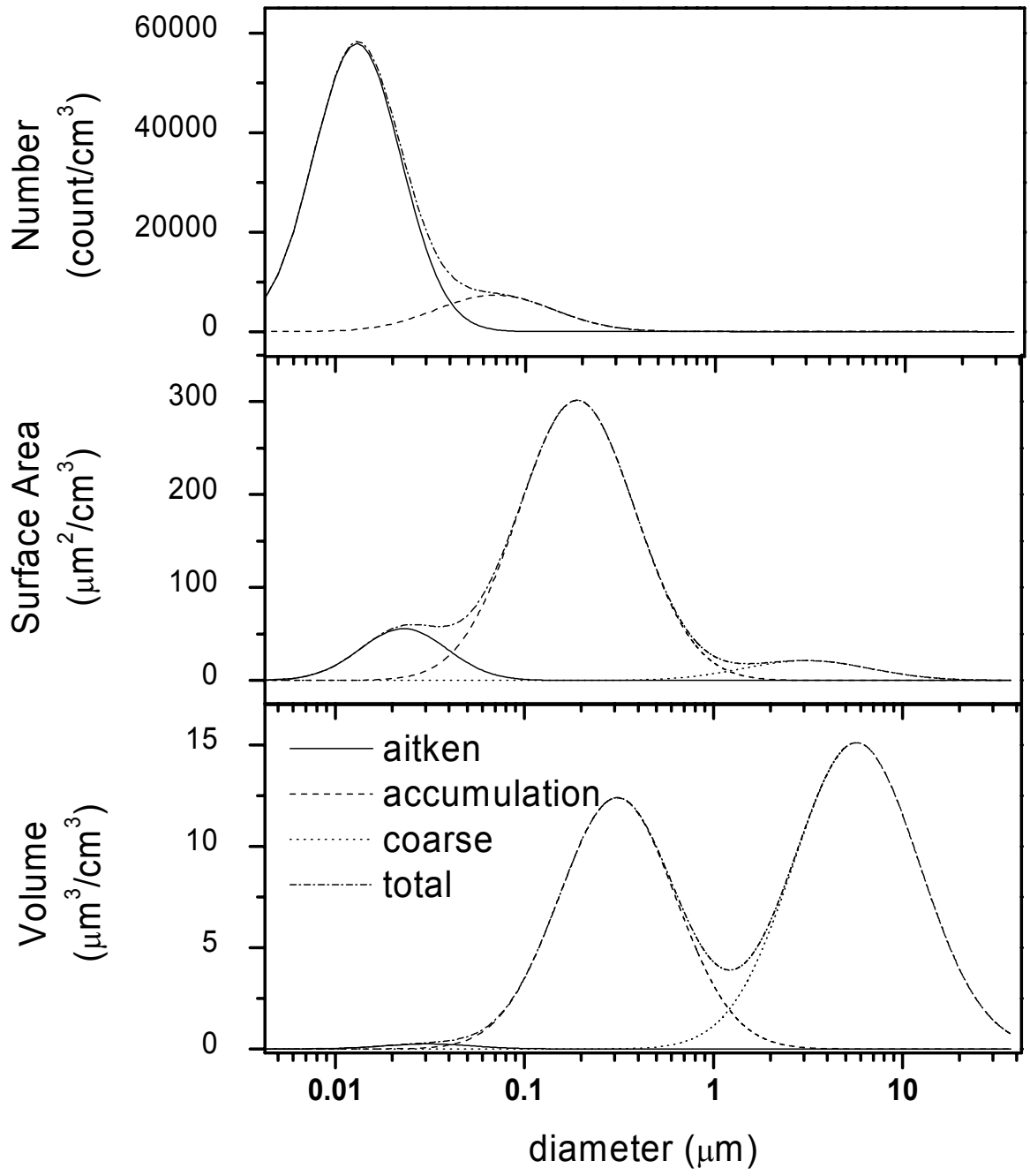


Figure 1.1: Atmospheric particle distributions by size, representative of typical urban distributions. Different panels represent different measurement parameters, which highlight different aerosol regions of interest. Different line styles represent different aerosol modes: aitken (solid), accumulation (dashed), coarse (dotted) and the sum of all three (dash-dot)[1,2].

### 1.1.1 Sources and sinks

Aerosols enter and leave the atmosphere in a variety of ways. Primary particles are emitted directly into the atmosphere. Examples of this include fine dust particles carried by wind or soot particles emitted during combustion. In contrast, other particles are produced by condensation of low volatility gases which are formed by photochemical reactions. These particles are called secondary aerosols.

The coarse particles shown in Figure 1.1 are mainly primary particles. These particles are produced largely by mechanical means and tend to settle from the atmosphere quickly, although recent work has shown that long range, intercontinental transport does occur under some conditions[1].

Fine particles are composed of a mixture of primary and secondary particles, the relative abundance of each depends on the region. Very small particles in the aitken nuclei mode, ranging from 10 to 80 nm, are formed by condensation of non-volatile or semi-volatile vapour. These droplets will coagulate with other particles, growing in size until they are ~ 1 μm. This growth by coagulation consumes smaller particles and creates the accumulation mode. Both the aitken nulei and the accumulation modes contain a large fraction of organic and inorganic compounds. The ultrafine mode was discovered as aerosol detection techniques improved. This mode consists of particles smaller than 10 nm and is of particular interest to researchers due to health effects[3].

The different modes have different removal methods as well as varied sources. Coarse mode particles are generally massive enough to be influenced strongly by gravity and will settle out in hours to days. Particles in the accumulation mode are longer lived, and will survive for days to weeks prior to removal by precipitation or sedimentation. Finally, aitken mode particles are consumed very quickly by coagulation: the residence time of these particles is usually less than an hour. A summary of the different aerosol modes, their sources and sinks is provided in Table 1.1.

Table 1.1: Aerosol properties, sources and sinks for different modes[4,5].

| | Aitken mode | Accumulation mode | Coarse mode |
|---|---|---|---|
| Size | 0.01 to 0.08 μm | ~1 μm | >2.5 μm |
| Sources | -Combustion<br>-Condensation of semivolatile organics<br>-Photochemical reactions producing non-volatile organics | -Combustion (soot and ash)<br>-Coagulation of Aitken nuclei<br>-Cloud aerosol evaporation | -Windblown dust<br>-Industrial emissions<br>-Biological particles |
| Sinks | -Coagulation<br>-Capture by cloud particles | -Precipitation<br>-Sedimentation (minor) | -Precipitation<br>-Sedimentation |
| Residence Time | < 1 hour | Days to weeks | Hours to days |

The research in this thesis focuses on larger particles of ~10 μm containing a mixture of organic and inorganic components. The composition of these particles is similar to particles in the accumulation mode, although larger due to limitations within our experimental apparatus.

### 1.1.2 Composition

The myriad of sources and reactions leading to typical atmospheric aerosols often leads to very complex composition[1]. Components of aerosols also tend to change with particle age, many organics become oxidized or react photochemically over time[6-8]. Both inorganic and organic components exist within typical atmospheric aerosols. The inorganic components have been relatively well characterized and consist mainly of sulfate, nitrate, chloride, ammonium and sodium[9]. The organic fraction of aerosols is much more complex and hundreds or thousands of different compounds have been identified as components. These compounds cover an extremely broad range of functionality, including carboxylic acids, alcohols, and polycyclic aromatic hydrocarbons (PAH)[10]. A significant amount of the organic fraction is also water soluble[11]. The relative quantities of each component vary substantially with location and sources, the organic fraction accounts for 18-70% (by mass) while sulfate (10-67%) and ammonium (6.9-19%) also make up substantial fractions of particle mass [9]. Atmospheric particles can also contain a variety of refractory components, including several types of mineral dust and soot particles.

A summary of fine particle compositions for urban (Figure 1.2) and rural continental (Figure 1.3) areas is provided below. These figures are adapted from a comprehensive field review by Zhang (and studies therein)[9].

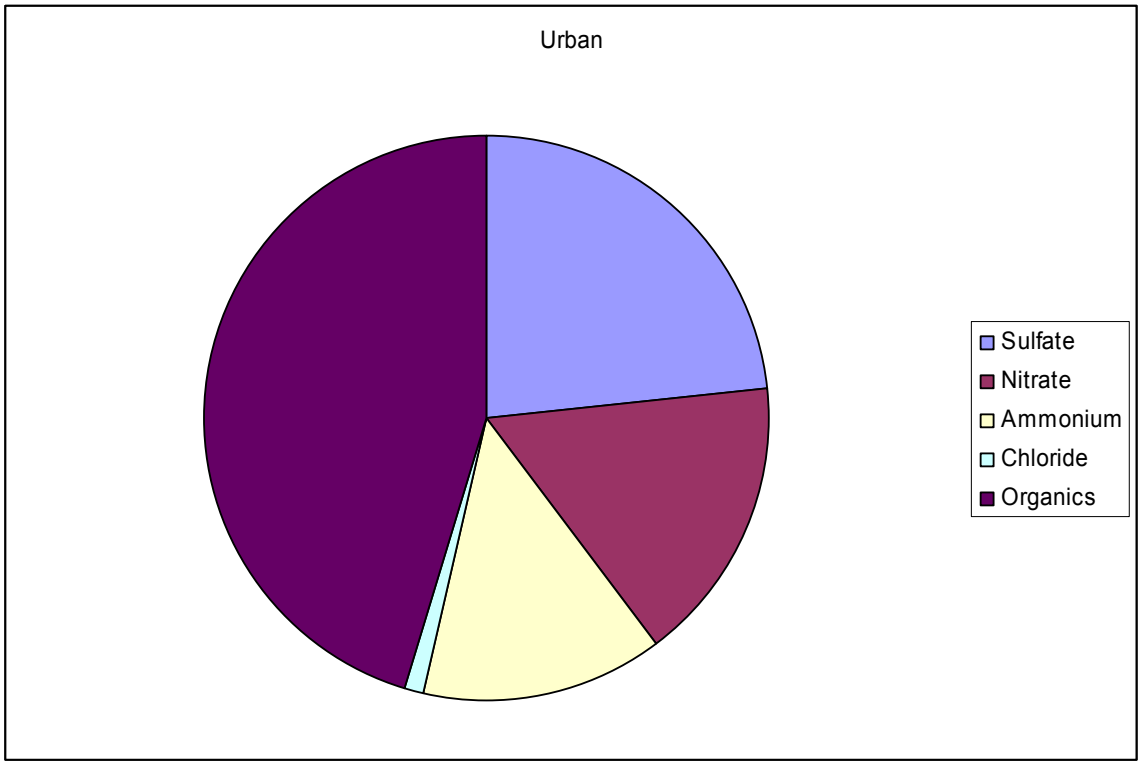


Figure 1.2: Average composition of aerosols from urban sites from Zhang et al[9]. Average loading is 17 μg/m$^3$ (though extreme cases are much higher, Beijing's measurements show aerosol loadings of 72 μg/m$^3$).

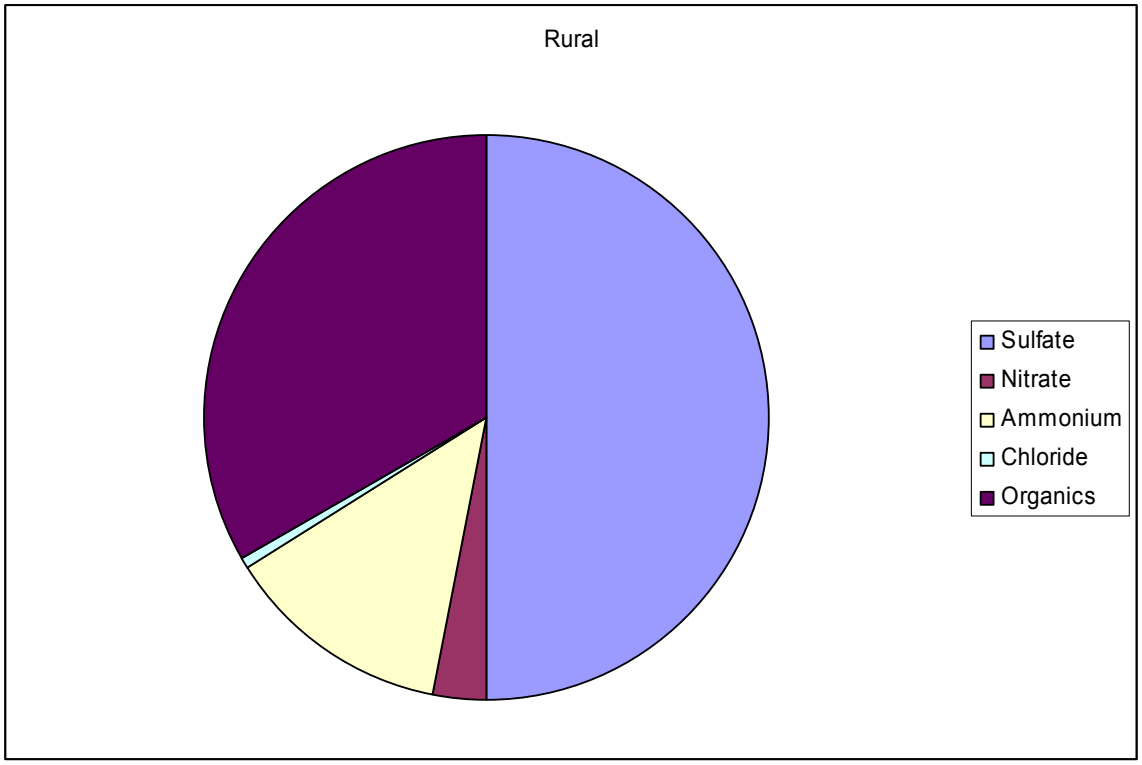


Figure 1.3: Average composition of aerosols from a variety of rural sites from Zhang et al[9]. Average loading is 8.2 µg/m3, though some measurements are much lower.

The previous figures apply to ground level aerosols. As the altitude changes so does the composition of aerosols. Froyd and Murray[12] investigated particle composition at a range of altitudes up to the lower stratosphere. The ratio of organic to organic + sulfate ranges between 0.3 and 0.8 in the troposphere, with a wider range observed below 5 km. This observation underlines the importance of investigating sulfate-organic mixtures, especially at temperatures and mass fractions relevant to the upper troposphere and stratosphere.

An additional consideration which is important when considering a group of atmospheric aerosols is the mixing state. Early field studies investigated aerosol components using various off-line analysis methods on filters[13]. In these experiments it was not clear whether individual particles contain all components (are internally mixed) or whether the particles are pure components and the measurements simply reflect the ratio of components (called external mixing)[14-16]. Figure 1.4 illustrates the difference between internal and external mixing states. Refinement of field study measurements using individual particle mass spectrometry has shown that many particles are internally

mixed, emphasizing the importance of studying mixtures in addition to individual component aerosols.

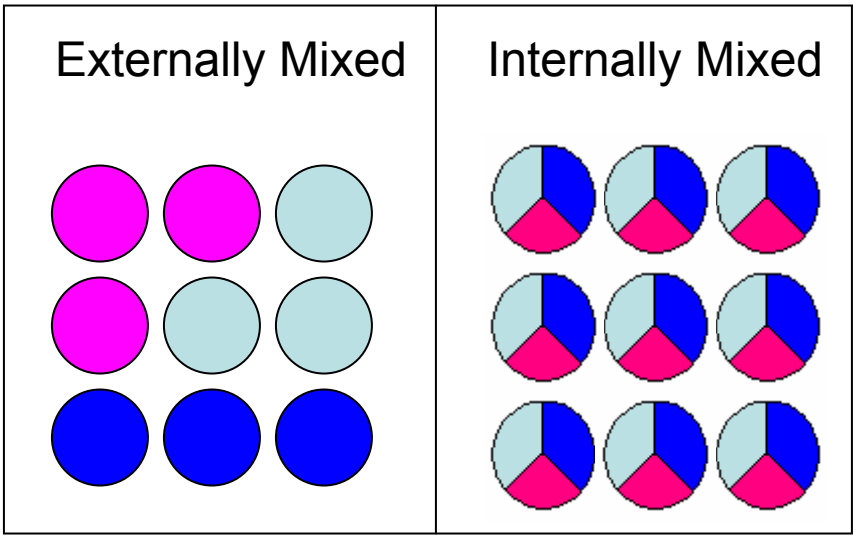


Figure 1.4: The different colours represent different components. The left panel shows a group of externally mixed aerosols while the right shows internally mixed aerosols.

## 1.2 Motivation for studying aerosols

Aerosols play a large role in human health[17], environmental policy[3,17], atmospheric reactivity[18,19], visibility[20] and climate[21]. The health effects associated with aerosols have been shown epidemiologically[3,22,23] and are due mainly to small (<1 μm) particles which get trapped deep in the respiratory system causing a wide range of health issues; from allergic reactions to cardiovascular diseases. The visibility effects associated with aerosols are caused by the scattering of light. Particles between 0.1 and 1 μm are responsible for the majority of atmospheric visibility reduction, because within this size range Mie scattering is most efficient[20]. In air with no particles or absorbing gases visibility could easily exceed 100 km, the visibility decreases rapidly as aerosols are introduced. Concentrations of 100 μg/m$^3$ have significant effects on visibility; an air mass with this concentration of particles (0.5 μm diameter) would reduce the visibility of otherwise clean air to just below 10 km[20].

Aerosols also have a substantial impact on the global radiation budget. By reflecting and/or absorbing incoming and outgoing radiation, aerosols can strongly influence the heating or cooling of the planet. The direct aerosol effect describes the

scattering and absorption by the particles themselves, dependent on particle size, composition and morphology. The indirect effect describes the ability of a particle to act as a cloud condensation nuclei (CCN) or ice nuclei (IN). The clouds formed in this way can then have additional effects on radiation. These two effects are the largest source of uncertainty in atmospheric models and climate predictions[21].

Atmospheric chemistry can also be influenced by the presence of aerosols. A tropospherically relevant case is the hydrolysis of $N_2O_5$, which has been shown to be most efficient on liquid droplets[18,19]. The variety in the aerosol impacts underlines the multidisciplinary nature of this field and highlights the relevance of ongoing research.

## 1.3 Overview of work

This work investigates phase transitions of mixed inorganic-organic aerosols at low temperatures. Three phase transitions are investigated; efflorescence, deliquescence and liquid-liquid separation. Efflorescence is the formation of a crystalline particle from an aqueous droplet. Deliquescence, the reverse process, is the formation of an aqueous droplet from a crystalline particle. Finally, liquid-liquid phase separation is the formation of two liquid phases in a previously homogeneous liquid droplet. These phase transitions are believed to influence a wide range of particle characteristics, including diameter, composition, ice nucleating ability and optical properties. The mechanism and physical chemistry involved in these processes is investigated in greater detail in the following chapters.

Chapter 2 will provide an overview of the physical chemistry underpinning the phase transitions investigated in this work. Chapter 3 provides a description of the efflorescence and deliquescence behaviour of citric acid and ammonium sulfate mixtures. Chapter 4 investigates the phase transitions of mixtures of 4-hydroxy-3-methoxy mandelic acid (HMMA) and ammonium sulfate. Finally, Chapter 5 will provide an overview of the research findings, conclusions and suggestions for future work.

# 2 Background and Theory

This thesis focuses primarily on three different phase transitions, liquid-liquid phase separation, efflorescence and deliquescence. The composition and temperature of aerosols greatly influences these phase transitions and thus, the physical state of the particle. This section examines efflorescence, deliquescence and liquid-liquid phase separation, focusing on binary or ternary systems. These systems are simplified examples of the complex mixtures which have been observed in the atmosphere but are useful as first steps toward understanding phase transitions in atmospheric aerosol particles.

The phase of the particle (i.e. liquid, solid, or mixtures of these) depends strongly on the water content of the aerosols and the water vapour immediately surrounding them. There are several different ways to quantify the amount of water vapour; relative humidity (RH) will be used throughout this thesis and is defined as

$$\frac{RH\,(T)}{100\%} = \frac{P_w}{P_{w\,sat}(T)}, \tag{2.1}$$

where $P_w$ is the partial pressure of water vapour in the gas, $P_{w\,sat}\,(T)$ is the partial pressure of water vapour over bulk water at temperature, $T$.

## 2.1 Efflorescence

Consider an aqueous particle containing a mixture of ammonium sulfate and liquid water, surrounded by a gas of known RH. As the RH is lowered, the particle will release water to remain in equilibrium with the surroundings and the diameter of the particle will change accordingly. Eventually, at a low RH (between 30% and 40% for ammonium sulfate), the dissolved salt will crystallize and the remaining aqueous water will be driven into the gas phase. This transition is known as efflorescence and occurs at the efflorescence relative humidity (ERH). It can be characterized by a sudden decrease in particle diameter (it can also be detected by changes in visible light scattering or spectroscopically). Figure 2.1 illustrates efflorescence for a typical ammonium sulfate-water mixture. The amount of aqueous water can be used to describe particle growth due to water uptake, values in this figure are obtained from the AIM thermodynamic model[24-27].

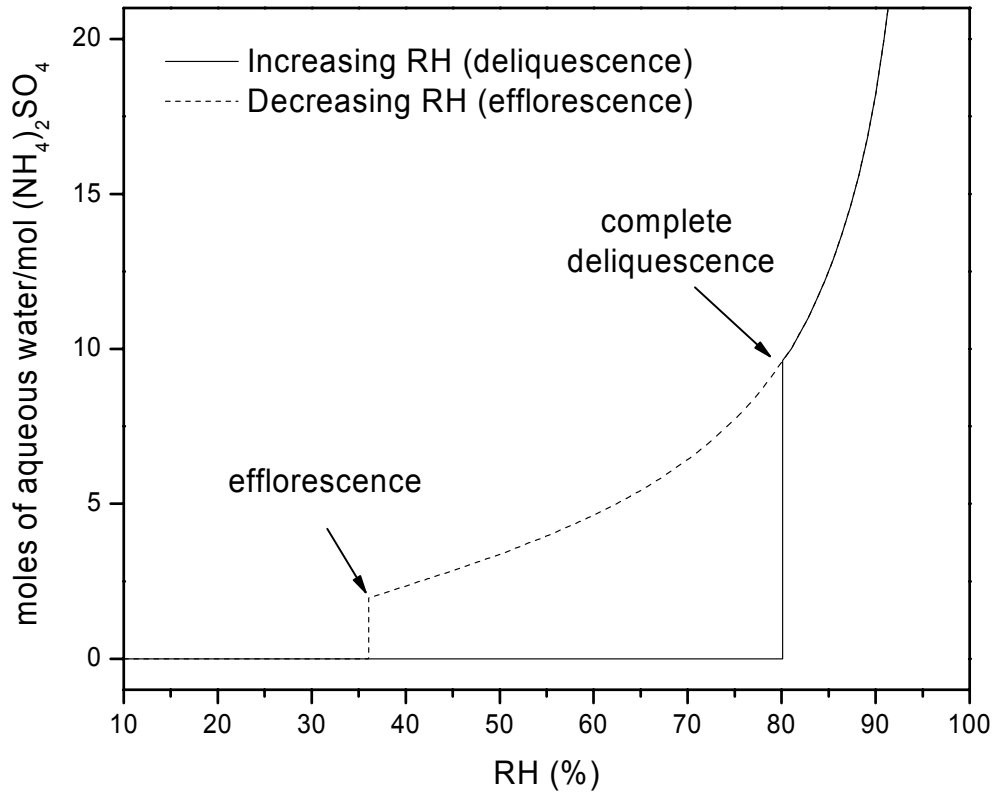


Figure 2.1: The hysteresis effect of ammonium sulfate-water mixtures is shown by the difference between efflorescence and deliquescence. Deliquescence is described in further detail in Section 2.3. Data modeled using e-AIM[27] for a binary system of ammonium sulfate and water at 293 K.

## 2.2 Classical nucleation theory:

Efflorescence behaviour can be better understood using classical nucleation theory (CNT). Under typical conditions, formation of an active nuclei of the salt is much slower than growth of the salt crystal inside an aerosol. Thus nucleation is the rate limiting step in most atmospheric aerosols. Here efflorescence and CNT is discussed using an ammonium sulfate-water system as an example. In this case only ammonium sulfate (the inorganic salt) can effloresce. Additional information and complete derivations are available in these references[28-30] with the bulk of the original theory described by Volmer[31], Gibbs[32] and Becker and Doring[33].

The central idea of CNT is that within a liquid body, a number of molecules spontaneously arrange into an ordered, very small embryo, which can initiate crystal growth. The formation of this stable embryo is an energy intensive process and many of the rearrangements in the liquid will not lead to a nucleation event, instead redissolving into the bulk liquid phase. It is helpful to discuss the formation of embryonic clusters in terms of the change in Gibbs free energy ($\Delta G$). The total change in free energy for the formation of an embryo is a combination of the energy gained by the new bulk phase, represented by $\Delta G_v$ and the energy required to form a new interface between the bulk liquid and newly created phase, $\Delta G_s$. This can be represented by

$$\Delta G = \Delta G_V + \Delta G_S , \tag{2.2}$$

where

$$\Delta G_V = \frac{4}{3}\pi r^3 \left(\mu_{solid} - \mu_{aqueous}\right) \tag{2.3}$$

and

$$\Delta G_s = 4\pi r^2 \gamma \tag{2.4}$$

and $\gamma$ is the interfacial surface energy between the embryo and bulk, $\mu_{solid}$ is the chemical potential of the embryo and $\mu_{aqueous}$ is the chemical potential of the surrounding bulk liquid. It is important to note that $\mu_{aqueous} > \mu_{solid}$ so the $\Delta G_v$ will be negative.

$\Delta G_v$ is proportional to the cluster volume ($r^3$) and negative, while $\Delta G_s$ is proportional to the cluster surface area ($r^2$) and positive. It is possible to calculate the critical radius of an embryonic cluster ($r_{crit}$) and the change in free energy associated with the creation of a nucleus of critical size ($\Delta G_{crit}$), which can be interpreted as the energy barrier to nucleation. Figure 2.2 has a qualitative representation of this behaviour.

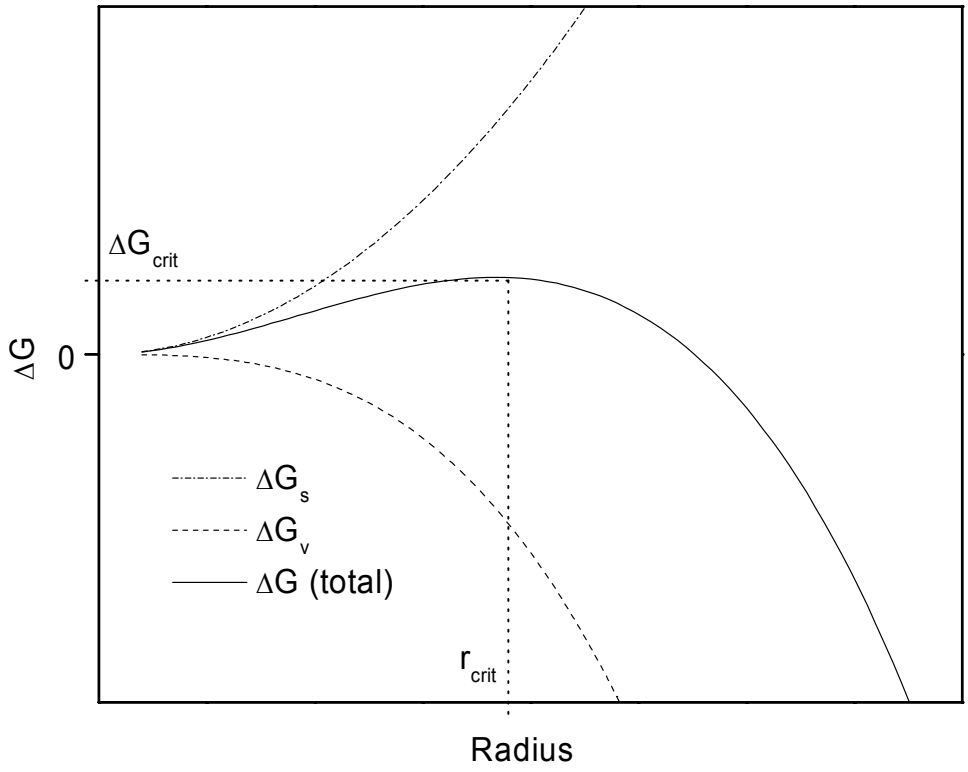


Figure 2.2: Change in Gibbs free energy for formation of a crystalline embryo, $\Delta G_{crit}$ is the energy barrier to form a nucleus of critical radius $r_{crit}$.

The change in free energy to create a nucleus of critical size ($\Delta G_{crit}$) is generally expressed in terms of supersaturation of the crystallizing phase using the Gibbs-Thomson relationship. The final form of the equation is

$$\Delta G_{crit} = \frac{16 n \pi \gamma^3 \nu^2}{3(\mathrm{k}T \ln S)^2}, \qquad (2.5)$$

where γ is the interfacial tension of the cluster, ν is the molecular volume, $S$ is the supersaturation of the crystallizing component, $n$ is the total number of ions for a dissociating compound ($n$ = 3 for ammonium sulfate, $n$ = 1 for non-electrolytes) and $k$ is the Boltzmann constant. The supersaturation term represents a ratio between the concentration and the saturated concentration. "Saturated" is the point where the salt would crystallize thermodynamically if there were no kinetic barriers; this is highly

temperature dependent. Since the crystallizing component is metastable (since it is supersaturated), the concentration exceeds the saturated concentration. Finally, expressing the concentration in terms of the activity coefficient makes using results from theoretical models easier. *S* is defined for dissolved ammonium sulfate as

$$S = \frac{a_{NH_4}^2 M_{NH_4}^2 a_{SO_4} M_{SO_4}}{\left(a_{NH_4}^2 M_{NH_4}^2 a_{SO_4} M_{SO_4}\right)_{sat}}, \tag{2.6}$$

where $a_n$ is the activity coefficient of component *n* (this is sometimes represented by γ in the literature, but since that term represents interfacial energy we have selected *a*), $M_n$ is the molarity of component *n* and the subscript *sat* represents the saturation case.

Once $\Delta G_{crit}$ is known it is a simple matter to calculate the rate of nucleation using the Arrhenius equation,

$$J = A \exp\left(-\frac{\Delta G_{crit}}{\mathrm{k}T}\right), \tag{2.7}$$

where *J* is the rate of nucleation and *A* is a pre-exponential factor. Thus the total rate of nucleation can be described as.

$$J = A \exp\left(\frac{16\pi\gamma^3 v^2}{3(\mathrm{k}^3 T^3 (\ln S)^2}\right). \tag{2.8}$$

This relationship has been applied to several efflorescing systems[34,35] and is used in Chapter 3 with an additional modification to address higher viscosities. It should be noted that it is only valid for systems where the crystal growth is much faster than nucleation, however this is generally true.

Until this point, the discussion has focused exclusively on a binary (water-inorganic) example, however, CNT can be extended to multi-component aerosols. One important factor in studying complex aerosols is whether all of the components will effloresce; in the case where several different components of a solution will effloresce independently, the earlier nucleating compounds can heterogeneously nucleate other crystal phases (this occurs in KCl and NaCl mixtures for example)[36]. In the experimental studies which make up this thesis, we focus on ternary systems containing ammonium sulfate-water and one organic. The organics selected for these studies did not efflorescence in the experiments, so the only efflorescing species was ammonium sulfate.

The equations presented above are generally applicable to the systems studied, however, values for the constants are often difficult to obtain.

## 2.3 Deliquescence

Deliquescence is the sister process to efflorescence, in that it represents the shift from a crystalline aerosol to an aqueous one. Recall Figure 2.1, which again considers a two component water-ammonium sulfate system. As the crystalline particle was exposed to increasing RH, the particle experiences no growth until a specific RH (~80%) and then suddenly increases dramatically in size due to water uptake. This phase transition is deliquescence and the humidity where it occurs is labeled the deliquescence relative humidity (DRH). Following this transition, the aqueous particle remains in equilibrium with the surrounding RH.

In order to understand why a crystalline particle deliquesces it is again useful to consider the Gibbs free energy of the system. According to thermodynamics, a system prefers to exist in the state with the minimum Gibbs energy. For the crystalline salt, the free energy $G_{(NH4)2SO4,solid}$, is constant but this is not true of the aqueous salt solution, $G_{(NH4)2SO4,aqueous}$. The Gibbs free energy of an aqueous ammonium sulfate solution depends on the activity of the salt in solution. At higher RH values the solutions becomes more dilute and the $(NH_4)_2SO_4$ activity is reduced, lowering $G_{(NH4)2SO4,aqueous}$. At the DRH the two energies are equal and at any RH exceeding the DRH $G_{(NH4)2SO4,aqueous} < G_{(NH4)2SO4,solid}$, this results in the formation of the solid shown in Figure 2.3. It follows that when the RH < DRH, then $G_{(NH4)2SO4,aqueous} > G_{(NH4)2SO4,solid}$.

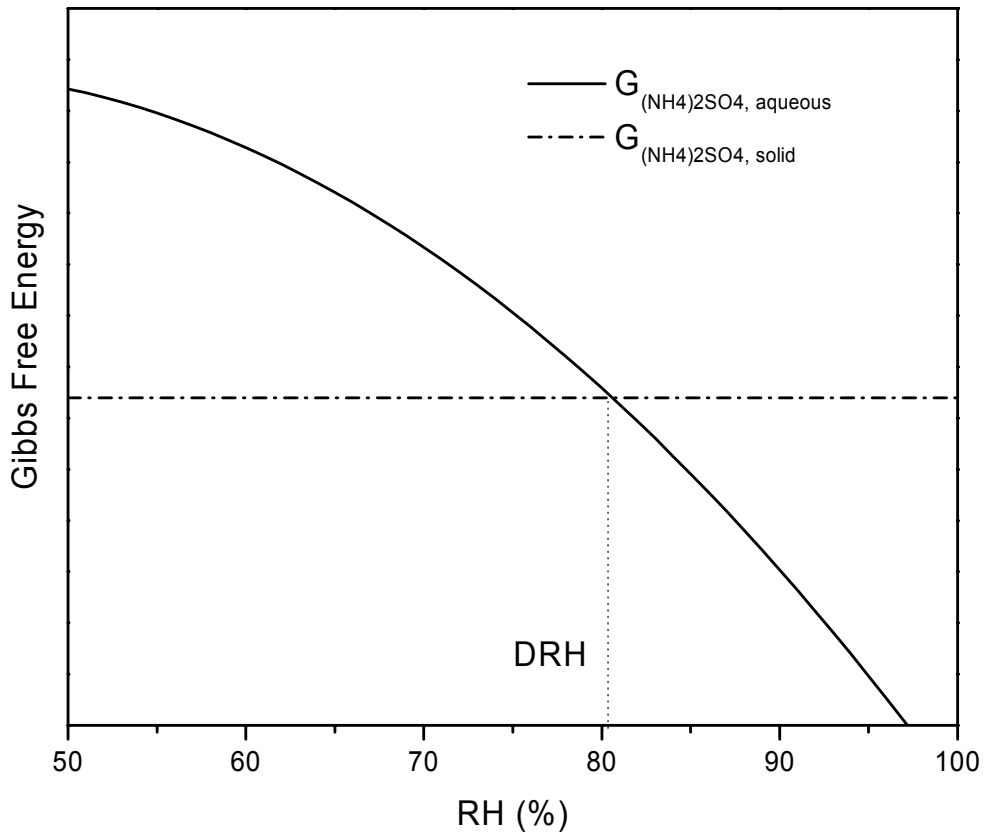


Figure 2.3: Gibbs free energy of an aqueous solution and solid salt as they vary with RH. At the DRH the energy of both states is equal (data from Seinfeld[37]).

Figure 2.3 highlights a subtle but extremely important difference between efflorescence and deliquescence. As discussed above, efflorescence is limited by the nucleation rate while deliquescence will generally occur as soon as it is thermodynamically favourable to do so. This difference leads to a hysteresis effect and has significant impacts on the physical state of atmospheric particles.

This discussion of a binary inorganic-water system applies equally well to a three component system, like those studied in this thesis (water-ammonium sulfate-organic). In the event that only one component deliquesces (as in our experiments), the remaining component(s) still influence water uptake[38]. Typically additional hygroscopic compounds will begin to uptake water earlier and more gradually, Figure 2.4 provides an example of

this behaviour. This behaviour can be contrasted with the less gradual behaviour of a binary water-inorganic system shown in Figure 2.1.

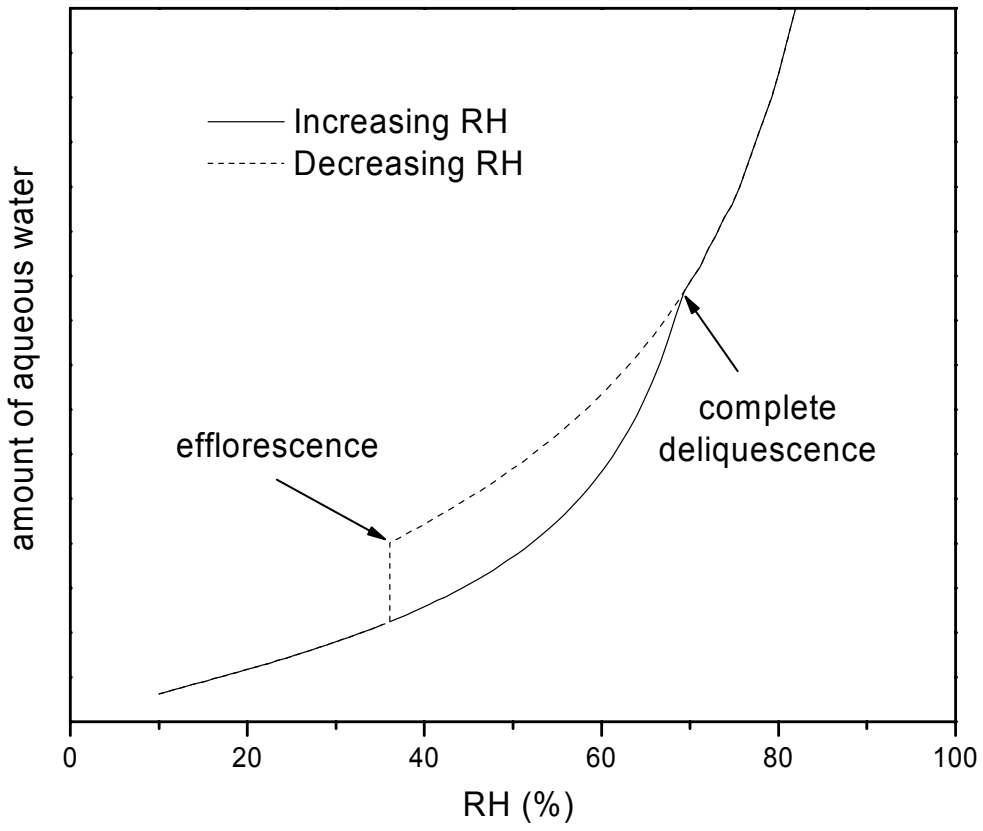


Figure 2.4: The addition of non-efflorescing organic components prompts earlier, more gradual water uptake relative to pure ammonium sulfate. Data obtained from an ammonium sulfate-organic-water mixture using e-AIM[27].

## 2.4 Liquid-liquid phase separation and salting out effects

Phase separation in atmospheric aerosols has not been explored in the same detail as efflorescence and deliquescence. Marcolli and Krieger[39] first demonstrated this class of phase transitions, although the idea that atmospheric aerosols may separate into an aqueous and organic phases predates this observation[40-42]. The formation of separate liquid phases in aerosols is related to the miscibility of the components. Early models of atmospheric behaviour (such as the AIM model developed by Clegg, Seinfeld and

Briscomb[24]) accounted for two liquid phases by assigning an aqueous and organic fraction with little mixing in between. This approach has been refined to allow detailed interaction and balancing of both phases with vapour and/or solid components as the models matured[25,26].

However, as investigated by Marcolli et al.[39,43] the addition of salt(s) to an organic-water solution influences the activity of all components and thus, their miscibility. The addition of a salt can increase a component's solubility, called "salting in", or decrease a component's solubility, called "salting out"[44,45]. These effects are well known in a variety of systems but had not previously been investigated in atmospherically relevant systems.

The salting in and out effects of electrolytes within liquid solutions has been studied extensively[46]. Several theories exist which adequately explain specific cases but a general explanation remains elusive. The complexity arises because there is substantial variety in the important interactions involved. These include interactions between species as well as self-interactions (eg. a water molecule interacting with other water molecules). Each of these interaction effects changes depending on the concentrations and properties of every component in solution, so extrapolation to complex systems can be difficult.

The salting out model which has been used to discuss atmospherically relevant systems in the literature is known as the hydration model[43]. The hydration model predicts that the salt ions interact preferentially with water (especially if the organic is nonpolar). As the amount of water decreases at lower RH there is not enough water to completely dissolve both the organic and salt ions, so the water and ions continue to interact while the organic phase separates and self-associates. This model is sufficient to explain the interactions observed to date, but may fail to account for differences in electrolytes and can not explicitly account for salting in effects.

## 2.5 Glass formation

A growing body of recent work has proposed that atmospheric aerosols may exist in a glassy, amorphous solid form. Glass transitions have been investigated in great detail for food applications, polymer systems and natural systems, but have only recently been discussed in terms of atmospheric implications.

Briefly, glass formation (also called vitrification) is a second order phase transition where a supercooled liquid is kinetically trapped into an amorphous solid phase rather than crystallizing into a solid with long range order. This is illustrated in Figure 2.5, and it is worth noting that the formation of a glass is never the most thermodynamically stable configuration. The reason that glass formation occurs in systems is that the system cools too rapidly for a long range order to form[29]. This occurs when either the cooling rate is fast or the viscosity of the system is high.

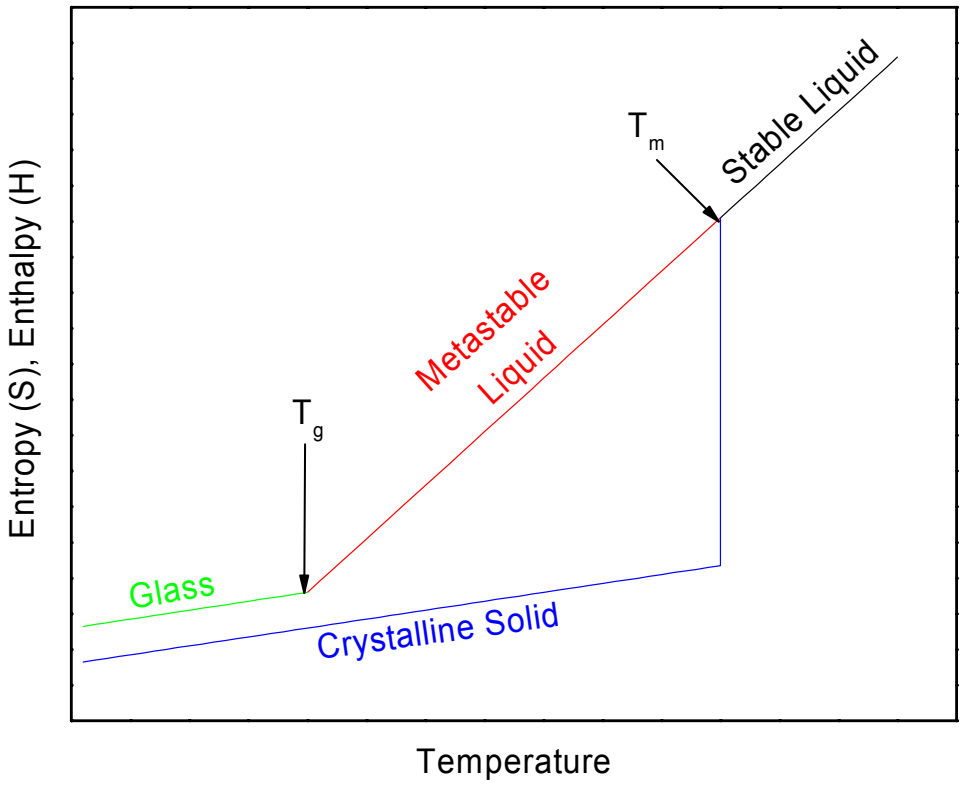


Figure 2.5: The thermodynamics associated with the glass transition are connected to temperature. As temperature decreases a stable liquid will either crystallize or remain a metastable liquid, eventually forming a glass. Tm is the melting temperature and Tg is the glass transition temperature.

The glass transition temperature is generally measured by differential scanning calorimetry (DSC), an experimental process where the heat flow required to keep both a

sample and reference at a controlled temperature is measured. Further discussion of the applicability of glass transitions to atmospheric aerosols is given in Chapter 3.

# 3 Inhibition of Efflorescence in Citric Acid-Ammonium Sulfate Particles < 250 K

## 3.1 Introduction

Measurements show that both organic and inorganic material are abundant in atmospheric aerosols[9], with the ratio of organic species to inorganic material depending on location, aerosol source and season. In addition, single particle measurements suggest that the dry organic mass fraction, organic/(organic+sulfate), in the upper troposphere ranges from 0.3 to 0.8 with more variation below 5 km. There is also abundant data from single particle measurements that show that organic and inorganic material are often internally mixed in the same particle[12,16,47]. These internally mixed organic-inorganic particles can undergo a range of phase transitions including deliquescence and efflorescence.

Efflorescence occurs when an aqueous aerosol is exposed to a low relative humidity and the inorganic and/or organic components crystallize. The reverse process is deliquescence, where a crystalline particle exposed to a high relative humidity takes up water to form an aqueous droplet. Deliquescence is thought to be a thermodynamically controlled process and occurs at a higher relative humidity than efflorescence. Between the deliquescence relative humidity (DRH) and efflorescence relative humidity (ERH) is a metastable region where particles can be crystalline, partially crystalline, or aqueous droplets, depending on their history. Recent work has shown that in most cases the organic component in the mixed organic-inorganic particles will not effloresce since the concentration of any one organic species is small[48]. The inorganic component, however, can deliquesce and effloresce.

Understanding and predicting the deliquescence and efflorescence properties of mixed organic-inorganic particles may be important for several reasons. For example, laboratory studies have shown that $N_2O_5$ hydrolysis is more efficient on aqueous deliquesced particles compared to effloresced particles[18,19]. In addition, effloresced particles are smaller than the corresponding deliquesced particles and have different optical properties[47,49]. Modelling studies suggest that the hysteresis effect of sulfate can change the direct effect by as much as 16%[50].

Recently, several studies have focused on the deliquesce and efflorescence of mixed organic-inorganic particles[34,35,48,51-63]. To date, however, most of these studies have focused on temperatures around 293 K, and there has only been one study of the efflorescence properties of mixed organic-inorganic particles at temperatures less than 273 K[64]. While room temperature studies are useful for understanding the phase properties of atmospheric aerosols in the lower troposphere, information on the temperature dependence of these phase transitions are still needed for predicting the deliquescence and efflorescence properties of aerosol particles in the middle and upper troposphere. In the following we have investigated the efflorescence properties of mixed organic-inorganic particles at temperatures down to 233 K.

Low temperature ERH measurements may be especially important for predicting ice nucleation in the troposphere. Deliquesced particles (free of foreign nuclei such as mineral dust) can only form ice by homogeneous nucleation, whereas effloresced particles can potentially act as heterogeneous ice nuclei[64-69]. It has been shown that effloresced ammonium sulfate particles can act as good heterogeneous ice nuclei under certain conditions. These effloresced ammonium sulfate particles may compete with other effective ice nuclei in the atmosphere, and as a result, they could play an important role in climate and the aerosol indirect effect[67]. Closely related to the above, Jensen et al.[70] examined the properties of cirrus clouds at low temperatures in the tropical tropopause layer (TTL) and concluded that ice number concentrations, ice crystal size distributions and cloud extinctions were inconsistent with homogeneous nucleation. The authors suggested heterogeneous ice nucleation on effloresced ammonium sulfate particles as a possible mechanism to explain the in situ and remote-sensing measurements. Froyd et al.[71] also suggested heterogeneous ice nucleation on effloresced ammonium sulfate particles as a possible mechanism to explain the composition of residual particles from evaporated cirrus ice crystals near the TTL. This mechanism assumes that mixed organic-inorganic particles will effloresce in the TTL or upper troposphere.

There is some data that suggest that the efflorescence properties of mixed organic-inorganic particles may be different at low temperatures compared to 293 K. Studies by Mullin and Leci[72,73] more than 40 years ago have shown that the rate of nucleation in

concentrated citric acid aqueous solutions decreases at temperatures of 273 K[72], possibly due to an increase in viscosity at lower temperatures. The rate of efflorescence of mixed organic-inorganic particles may decrease at lower temperatures due to an increase in viscosity as well. In addition recent studies have shown that aqueous organic components[74,75] and aqueous organic-inorganic[75] particles can form glasses under atmospherically relevant conditions[76]. The formation of glasses should limit efflorescence. On the other hand, Wise et al.[64] studied mixed palmitic acid-ammonium sulfate particles at temperatures down to 245 K and found that insoluble palmitic acid had little effect on the efflorescence properties of ammonium sulfate.

In the following we study the efflorescence properties of mixed citric acid-ammonium sulfate particles as a function of temperatures. Citric acid (COOH-$CH_2$-COH(COOH)-$CH_2$-COOH, Molar Weight: 192.12 g/mol) contains three carboxyl groups (-COOH) and an alcohol group (-OH) and exists in the atmosphere in small quantities[11]. We also investigated the glass transition temperatures of mixed citric acid-ammonium sulfate solutions using a Differential Scanning Calorimeter (DSC) in order to relate efflorescence limitation to glass formation of the particles. Citric acid has recently been used as a model system to represent oxygenated organics in the atmosphere[74,76]. Also aqueous solutions of citric acid often form glasses at low temperatures[77,78]. Ammonium sulfate was chosen for these studies since it is an important inorganic species in the atmosphere. Also, for the conditions studied by Jensen et al.[70] discussed above, the sulfate was fully neutralized to ammonium sulfate, which was recently supported by single particle mass spectrometer data taken at the tropical tropopause[71].

## 3.2 Experimental

The technique used to study efflorescence has been described in detail elsewhere[35,58,79]. A brief overview is provided here with a focus on details specific to the current experiments. The system consists of an optical microscope (using polarized light) coupled to a temperature controlled flow cell. The bottom surface of the flow cell is a hydrophobic glass slide upon which the particles of interest are deposited and observed. Relative humidity in the cell was controlled by a continuous flow of a mixture of humid and dry $N_2$. Typical flow rates were approximately 1.5 L/min.

Efflorescence experiments were conducted at five temperatures ranging from 293 K to 233 K. During experiments the particles were first deliquesced by exposing them to an RH close to 100%. Next the humidity was reduced to approximately 50% RH in one step and then decreased by approximately 0.1 %RH/min for the remainder of the experiment. During the experiments, images were taken every 15 seconds by a camera coupled to the microscope. Particles ranged in size from 5-30 μm in diameter. For each particle, the efflorescence relative humidity (ERH) was considered to be the first appearance of solid in the particle, even if the particles appeared only partially crystalline.

Ammonium sulfate (Fisher, 99.8%) and citric acid (Sigma-Aldrich, 99+%) were used as supplied. Bulk mixtures were prepared gravimetrically and dissolved in millipore filtered water (18.2 MΩ). To prepare the particles the solution was passed through a nebulizer to produce submicron particles. These particles were directed towards a hydrophobic glass slide where they coagulated into supermicron droplets.

The compositions of particles and/or solutions are typically reported in dry mole fraction citric acid. This dry mole fraction is calculated as

$$X_{CA,dry} = \frac{n_{CA}}{n_{CA} + n_{AS}}, \tag{3.1}$$

where $X_{CA,\ dry}$ is the mol fraction of citric acid in a dry (containing no water) particle or solution, $n_{CA}$ is the moles of citric acid and $n_{AS}$ is the moles of ammonium sulfate. Keep in mind, however, that this does not imply the particles and solutions are completely dry. This nomenclature is used since it is a convenient method for representing the citric acid-to-ammonium sulfate ratio in particles and solutions.

Glass transition temperatures of different citric acid-ammonium sulfate-water solutions were performed in a commercial DSC (TA instruments Q10). In one set of experiments, the mass fractions of the total solutes (citric acid and ammonium sulfate) varied between 0.603 and 0.7916, whereas $X_{CA,dry}$ stayed constant at 0.7. In the second set of experiments, the total mass fraction of solutes was kept at roughly 0.6, whereas the $X_{CA,dry}$ was changed. All experiments were performed with bulk samples. Ammonium sulfate (Fluka, >99.5%) and citric acid (Fluka, >99.5%) were used as supplied. The glass

transition temperatures were determined as the onset of the heat signal in the heating cycle, and have accuracy in the absolute temperature of ±0.9 K[75].

## 3.3 Results

### 3.3.1 ERH of pure ammonium sulfate ($X_{CA,dry}$ = 0.0) vs. temperature

Prior to studying mixed organic-inorganic particles, we studied the efflorescence properties of pure ammonium sulfate particles as a function of temperature. This provided a reference point for the mixed organic-inorganic particles, as well as a way to validate our system for low temperature studies.

Measurements shown in Figure 3.1 (solid symbols) are our results for pure ammonium sulfate particles. The solid symbols refer to the average ERH. Since efflorescence is a stochastic process, all the particles did not effloresce at the same RH even for the same temperature. The error bars represent a combination of the range over which 95% of the particles efflorescence (2σ) as well as the uncertainty from measuring the relative humidity. The data suggest that efflorescence of ammonium sulfate between 293 K and 233 K is relatively insensitive to temperature; this trend follows closely the temperature trend for deliquescence of ammonium sulfate, which only varies by roughly 4% RH over 50 K[36]. Also included in Figure 3.1 are results from other groups that have studied the same temperature range. The previous studies include a range of different techniques including an electrodynamic balance (EDB)[80] where a particle is suspended in an electric field and aerosol flow tubes[81,82] where the particles are suspended in a gas flow. The good agreement between our measurements and previous measurements where particles were not in contact with a surface suggests that the hydrophobic support in our experiments do not significantly affect our efflorescence results, a conclusion that is consistent with previous studies from our laboratory[34,35,83] and other groups[60,84].

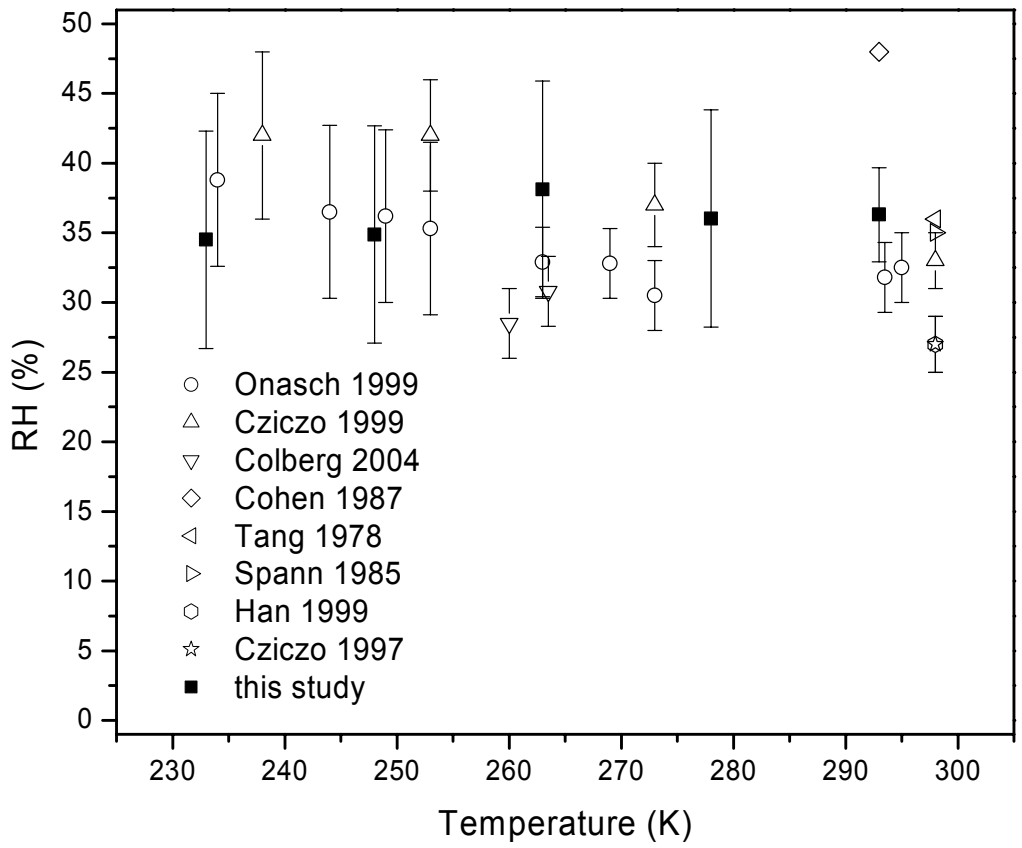


Figure 3.1: Measurements of the efflorescence of pure ammonium sulfate as a function of temperature. Filled squares are this study, unfilled symbols represent these references[80-82,85-88].

### 3.3.2 ERH of mixed ammonium sulfate-citric acid particles at room temperature

Shown in Figure 3.2 are our results for mixed ammonium sulfate-citric acid particles at room temperature. Similar to Figure 3.1, the symbols represent the average efflorescence relative humidity. For experiments where more than 20 particles were observed at a given concentration, the error bar corresponds to ± 2σ for the results as well as the uncertainty of the hygrometer(~1.1%). In cases where less than 20 nucleation events were observed the error bars correspond to ± 7.8%. This is a conservative estimate based on the maximum 2σ observed in our experiments where more than 20 nucleation

events were observed. Our results illustrate that the addition of citric acid slowly decreases the ERH of ammonium sulfate in the particles. At 0.25 mole fraction the decrease is approximately 10% RH. At 0.3 mole fraction the particles did not effloresce at all, even when exposed to our system's minimum RH (< 1%) for longer than an hour. Also shown in Figure 3.2 are results from other groups who studied the efflorescence of mixed citric acid-ammonium sulfate particles at room temperature. Choi[57] used an EDB to study a citric acid mole fraction of ~0.59. In these studies they did not observe crystallization, consistent with our measurements[57]. Zardini et al.[59] used both an EDB and hygroscopicity tandem differential mobility analyzer (HTDMA) to study efflorescence. All the data from Zardini et al. are in excellent agreement with our data except at $X_{CA,\ dry}$ = 0.2, where they see a slightly higher ERH than observed in our studies. When comparing the data sets a relevant parameter is the change in ERH when going from pure ammonium sulfate to $X_{CA,\ dry}$ = 0.2. Zardini observed a decrease in ERH between 0-3%; whereas, we observed a decrease between 2-15%. Considering the uncertainties in the measurements the differences between data sets appears to be relatively small.

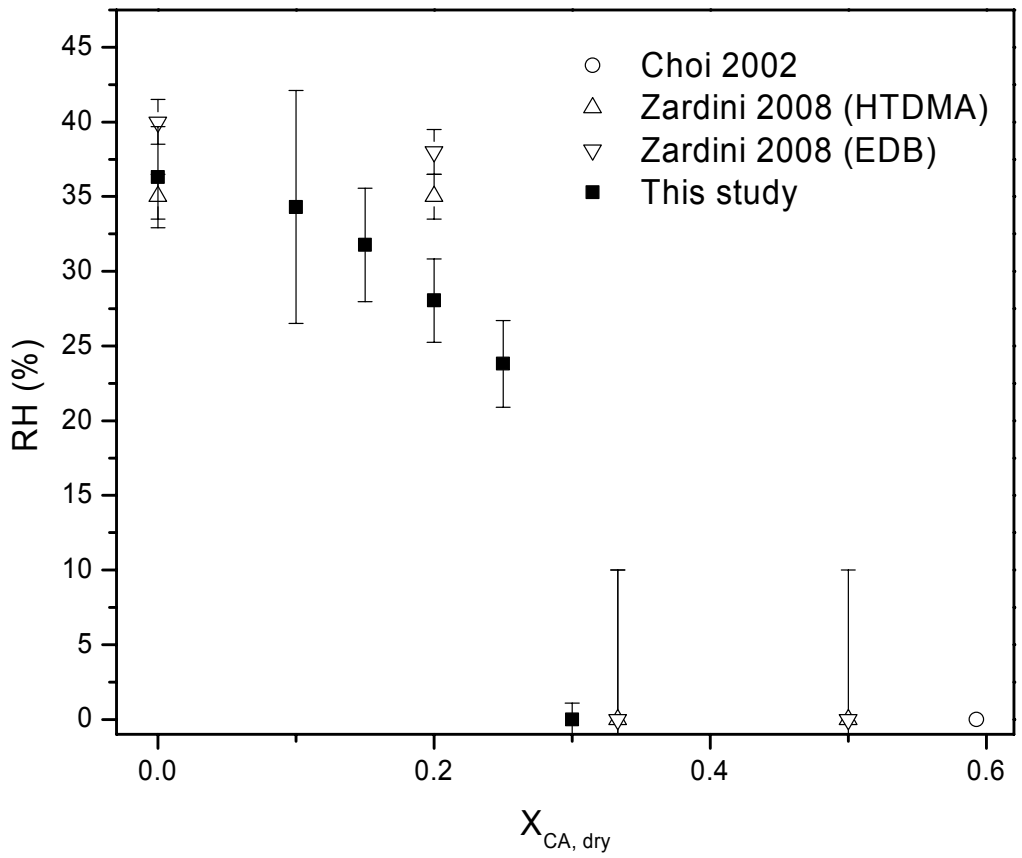


Figure 3.2: Efflorescence of citric acid-ammonium sulfate particles at room temperature. Filled squares represent this study, unfilled circles Choi[57], unfilled triangles are Zardini 2008. For compositions of 0.33 and 0.5 Zardini[59] did not observe efflorescence at RH values greater than or equal to an RH of 10%. Experiments were not carried out at RH values less than 10%, and the symbols and error bars at these compositions are used to indicate this fact.

The general trend illustrated in Figure 3.2 (decrease in efflorescence with addition of organic compounds) for citric acid-ammonium sulfate is consistent with the trends observed with systems containing other highly oxygenated organic species. To illustrate this point, we compare, in Figure 3.3, the results from our citric acid studies with previous measurements from our group which utilized a similar apparatus. Included in the figure are results for malonic acid, glycerol and leviglucosan[35]. The results illustrate that all systems have a similar trend, but there are significant quantitative differences

between the systems. For example at a mole fraction of 0.3 the citric acid system does not effloresce whereas the malonic acid system effloresces at 20.7% RH.

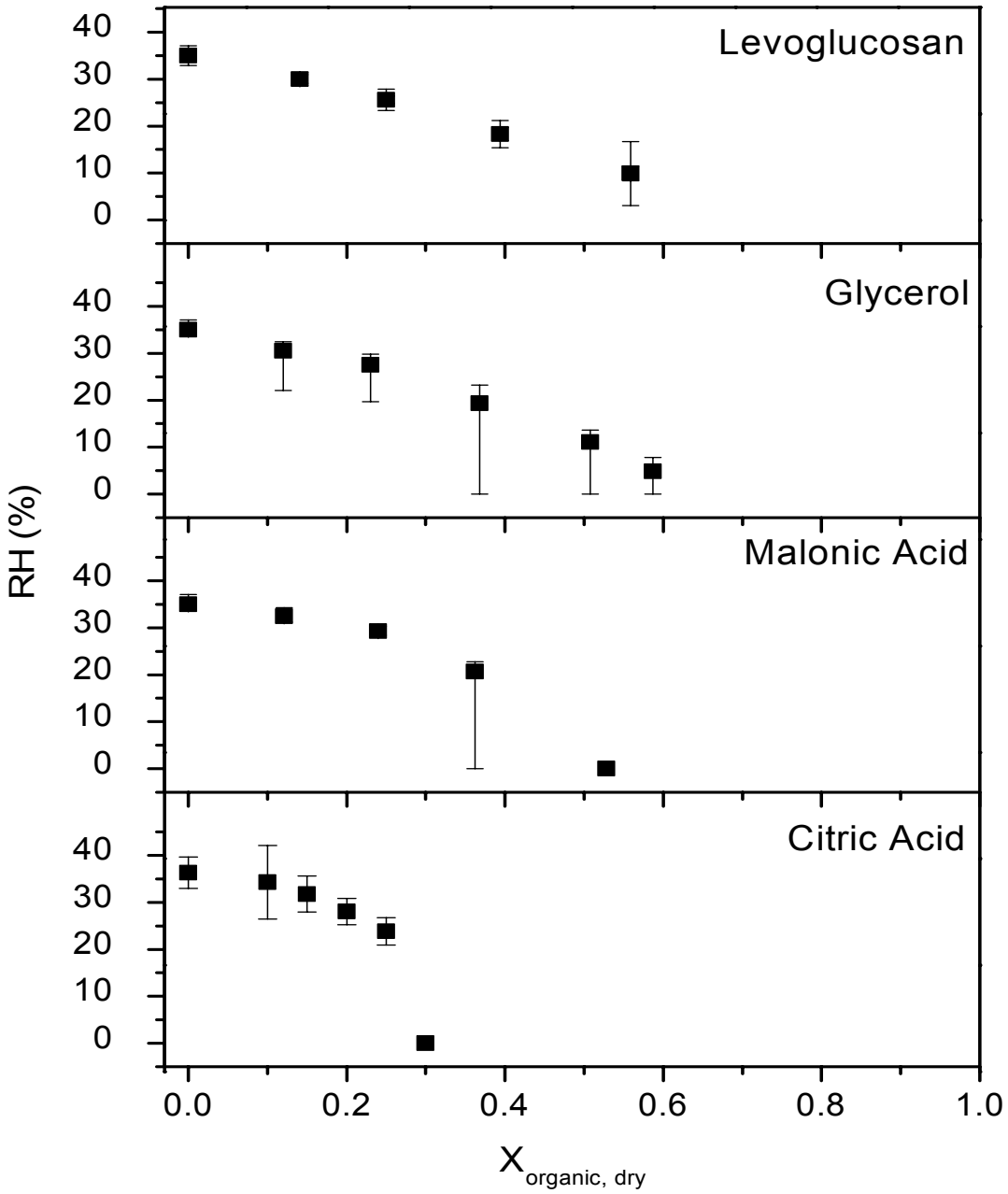


Figure 3.3: Room temperature comparison between citric acid (this study) and several organics studied previously in our laboratory[35].

The differences between systems shown in Figure 3.3 may be explained by classical nucleation theory. In our experiments, the efflorescence relative humidity is expected to be limited by the rate of homogeneous nucleation of ammonium sulfate in the particles. This is expected because the rate of crystal growth is almost instantaneous, based on observations of particles during efflorescence events. According to classical nucleation theory the rate of homogeneous nucleation of crystalline ammonium sulfate in the particles can be described by

$$J = A\exp\left[-\frac{16\pi\gamma^3 v^2}{3k^3T^3(\ln S)^2} + \frac{\Delta G'}{kT}\right], \tag{3.2}$$

where the nucleation rate, $J$, is the number of nuclei formed for a unit volume and time[28], $A$ is a pre-exponential factor, $k$ is Boltzmann's constant, $v$ is the molecular volume of ammonium sulfate, $T$ is temperature, $S$ is the supersaturation of crystalline ammonium sulfate, $\gamma$ is the interfacial energy between the embryo and the surrounding liquid and $\Delta G'$ is a molecular rearrangement term (which is strongly correlated to viscosity). As discussed previously, one possible explanation for the variation in efflorescence from system to system is that $\gamma$ varies significantly from system to system. This would lead to considerably different nucleation rates at a similar relative humidity since the surface tension is cubed. Another possibility is that at low RH, viscosity may become significant and vary from system to system at high mole fractions of organics. In this case, viscosity can limit the nucleation rate (through $\Delta G'$). A final possibility is that the degree of supersaturation at a given RH varies significantly from system to system due to non-ideal behavior.

### 3.3.3 ERH as a function of temperature

Figure 3.4 shows the efflorescence results for the five temperatures studied. Qualitatively, the trend observed at lower temperature remains the same, where increasing amounts of organic compounds cause a slight reduction in ERH followed by a complete inhibition. However, at 248 K and 233 K the efflorescence is inhibited at lower mole fractions; at 0.25 and 0.2 respectively. This suggests that at low temperatures efflorescence can be inhibited by smaller concentrations of citric acid.

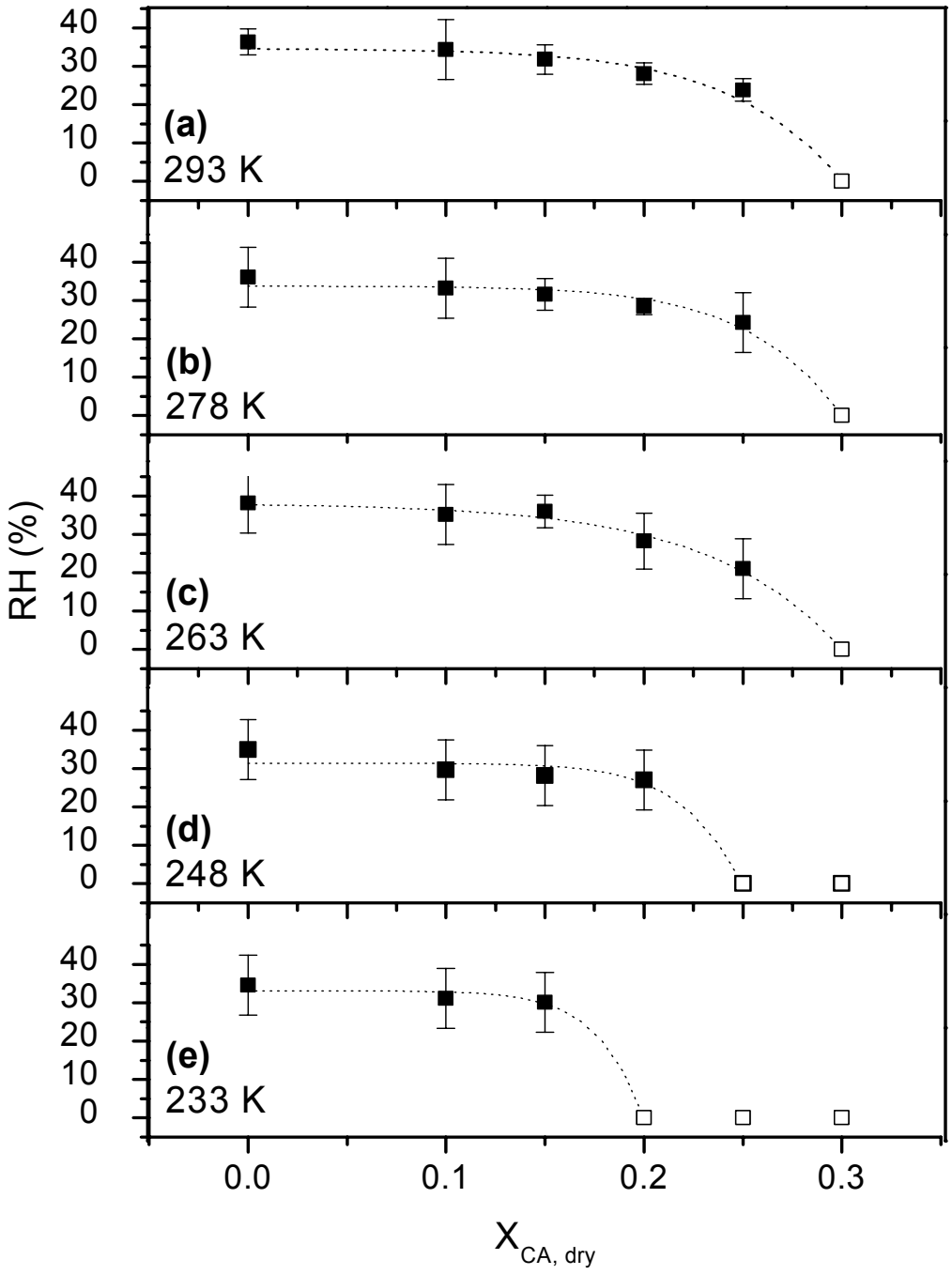


Figure 3.4: Efflorescence data for different dry organic mole fractions of citric acid-ammonium sulfate particles. Different panels represent different temperatures, solid points represent observed efflorescence events and unfilled points are non-efflorescing mixtures. The dashed line is included to help guide the eye.

Figure 3.5 shows the same data as Figure 3.4, replotted using RH and temperature as variables. This figure more clearly illustrates that the efflorescence for $X_{CA,\ dry}$ = 0.0, 0.1 and 0.15 is relatively insensitive to temperature. A linear fit for these three data sets shows slopes between 0.03 and 0.07 %RH/K. Figure 3.5 also illustrates that at $X_{CA,\ dry}$ = 0.2 and 0.25 the ERH is a strong function of temperature, with a sudden change in ERH at 233 K and 248 K for $X_{CA,\ dry}$ = 0.2 and 0.25 respectively. Similar to Figure 3.4, this shows that at low temperatures (< 250K) and high organic compound concentrations ($X_{CA,\ dry}$ = 0.2 and 0.25) efflorescence appears to be inhibited. Figure 3.5 also contains lines examining the glass transition temperature of the organic-inorganic mixtures, these are discussed in greater detail below.

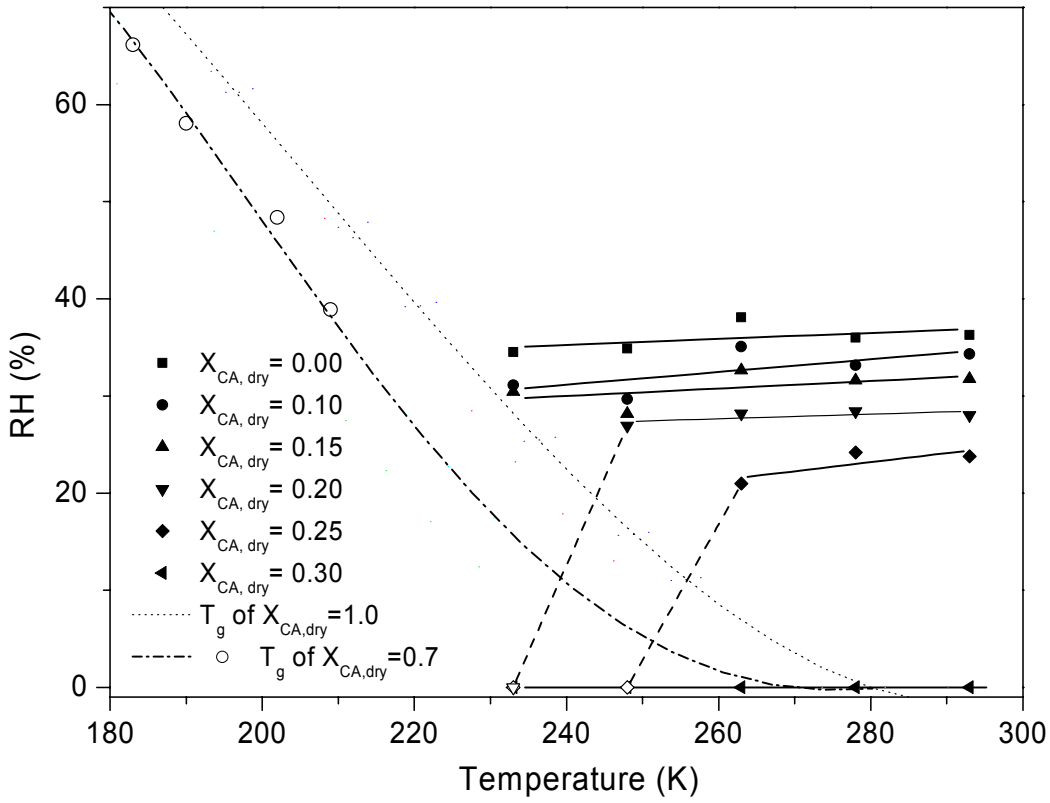


Figure 3.5: Efflorescence data from this study and calculated glass transition data (see text for further details). The dotted line represents the $T_g$ of a binary mixture of water and citric acid ($X_{CA,dry}$ =1.0). The dash-dot line and open symbols correspond to ternary mixtures with $X_{CA,dry}$ =0.7.

Recently in an elegant set of experiments, Wise et al.[64] studied the efflorescence properties of ammonium sulfate particles coated with palmitic acid down to approximately 245 K. These authors observed efflorescence at approximately 35% RH for the entire temperature range studied and noted that the organic coating had little effect on the efflorescence of ammonium sulfate. One likely reason for the difference between our results and the results by Wise et al. is the properties of the organic material studied. Palmitic acid is insoluble in water. On the other hand, citric acid is water soluble and does not crystallize under the conditions we explored.

### 3.3.4 Explanation of temperature dependence

Again, the temperature dependence of the ERH may be rationalized with classical nucleation theory and equation 2. One possible explanation for the efflorescence inhibition illustrated in Figure 3.4 and Figure 3.5 is that in the particles at lower temperatures which were rich in organics (0.20 and 0.25 mole fractions) do not reach as large a supersaturation with respect to ammonium sulfate ($S_{(NH4)2SO4}$), possibly due to non-ideal solution behaviour. As a result the driving force for efflorescence (i.e. $S$ variable in equation 3.2) is smaller at the lower temperatures and in the most concentrated particles. To explore this we calculated the $S_{(NH4)2SO4}$ reached in all experiments where efflorescence was observed using the e-AIM model[27]. These results are represented by solid symbols in Figure 3.6. Although e-AIM assumes that ion-organic component interactions are minor, it has been used to represent this system in 1:1 mole ratio previously with some success[89]. In general, supersaturations with respect to ammonium sulfate ranged from 30 to approximately 75. Next we calculated lower limits to the $S_{(NH4)2SO4}$ reached in the experiments where efflorescence was not observed. The results from these calculations are represented by the open symbols in Figure 3.6. To calculate these lower limits we used the e-AIM model and an RH of 10%. In the experiments where no efflorescence was observed $S_{(NH4)2SO4}$-values greater than 150 were reached which is clearly larger than the $S_{(NH4)2SO4}$-values reached in the experiments where efflorescence was observed. We conclude that a low $S_{(NH4)2SO4}$-value at the lowest temperatures and in particles with greater organic component loadings cannot explain our observations[24-26,90].

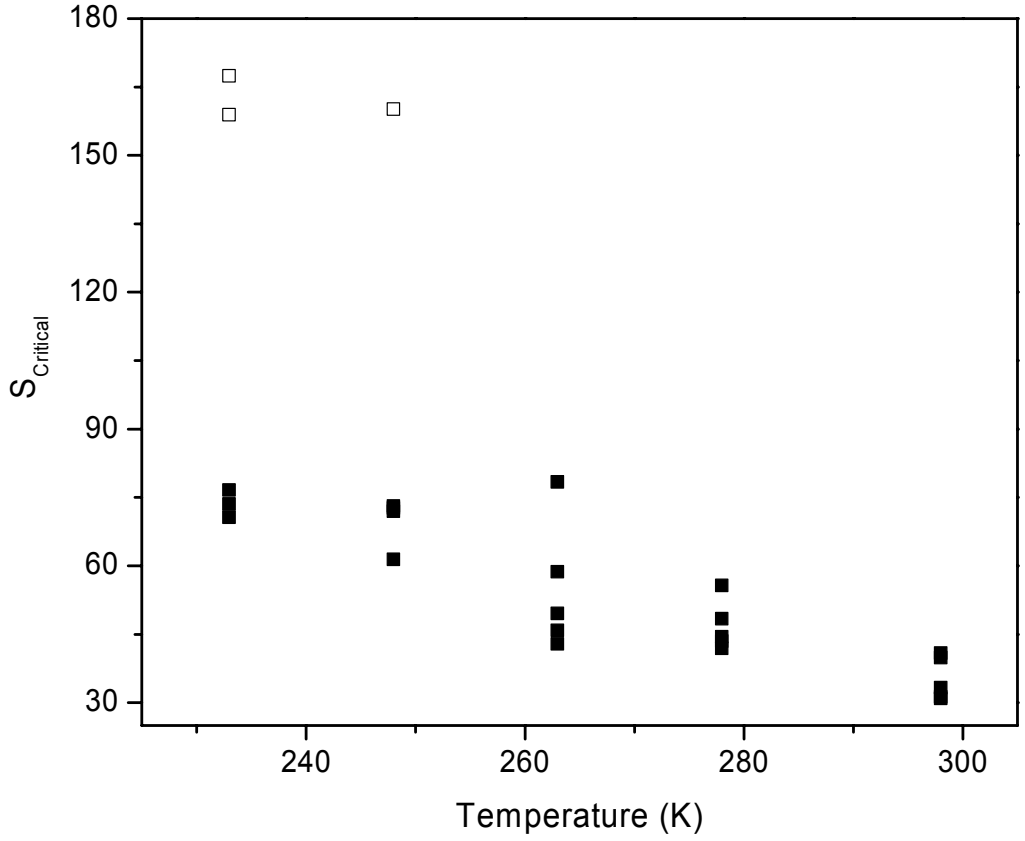


Figure 3.6: The supersaturation required to induce efflorescence, $S_{critical}$, observed in our experiments. The solid points correspond to observed efflorescence events while unfilled points represent the lower limit associated with non-efflorescing mixtures.

The inhibition trend at low temperatures observed in our experiments may be related to crystallization studies in aqueous citric acid solutions carried out 40 years ago[72]. The authors argued that the decrease in nucleation events at lower temperatures was due to an increase in viscosity which would increase $\Delta G'$ in equation 8. This can also explain the observed inhibition of efflorescence of mixed ammonium sulfate-citric acid particles at the lowest temperatures in our experiments.

### 3.3.5 Possible connections with glass transition temperatures

As mentioned in Section 3.1, recent work has shown that both fully organic particles and mixed organic-inorganic particles can form glasses at low temperatures of

atmospheric relevance[74,75]. Prior to our work there have not been any reports of glass transition temperatures of citric acid-ammonium sulfate-water solutions. Below we investigated the glass transition temperatures of these solutions using a DSC and relate these values to the observed efflorescence conditions.

Shown in Figure 3.5 and Figure 3.7 (solid symbols) are the glass transition temperatures, $T_g$, we determined for mixed citric acid-ammonium sulfate-water solutions. Each $T_g$ is a mean value of two single measurements. Note we were unable to measurement glass transition temperatures for a wider range of solute mass fractions or for different $X_{CA,dry}$-values since in these solutions either ice or ammonium sulfate crystallization was observed before reaching the glass state. The solid line through the square symbols is a parameterization of the experimental data for $X_{CA,dry}$ = 0.7 using the Gordon-Taylor equation[91]. Gordon and Taylor first postulated an equation which allows computing the glass transition temperature of aqueous solutions, $T_g$, as a function of the mass fraction of the solute, $w_2$. This equation takes the form

$$T_g(w) = \frac{w_1 T_{g1} + \frac{1}{k} w_2 T_{g2}}{w_1 + \frac{1}{k} w_2}, \qquad (3.3)$$

where $w_1$ is the mass fraction of water, $Tg_1$ and $Tg_2$ are the glass transition temperatures of pure water and of the solute, respectively. For $X_{CA,dry}$ values of 0.7 we fit the experimental data to this equation using $T_{g1}$ as 136 K[92,93]. The parameters from the fit are $T_{g2}$ = 273.6 K and $k$ = 4.383.

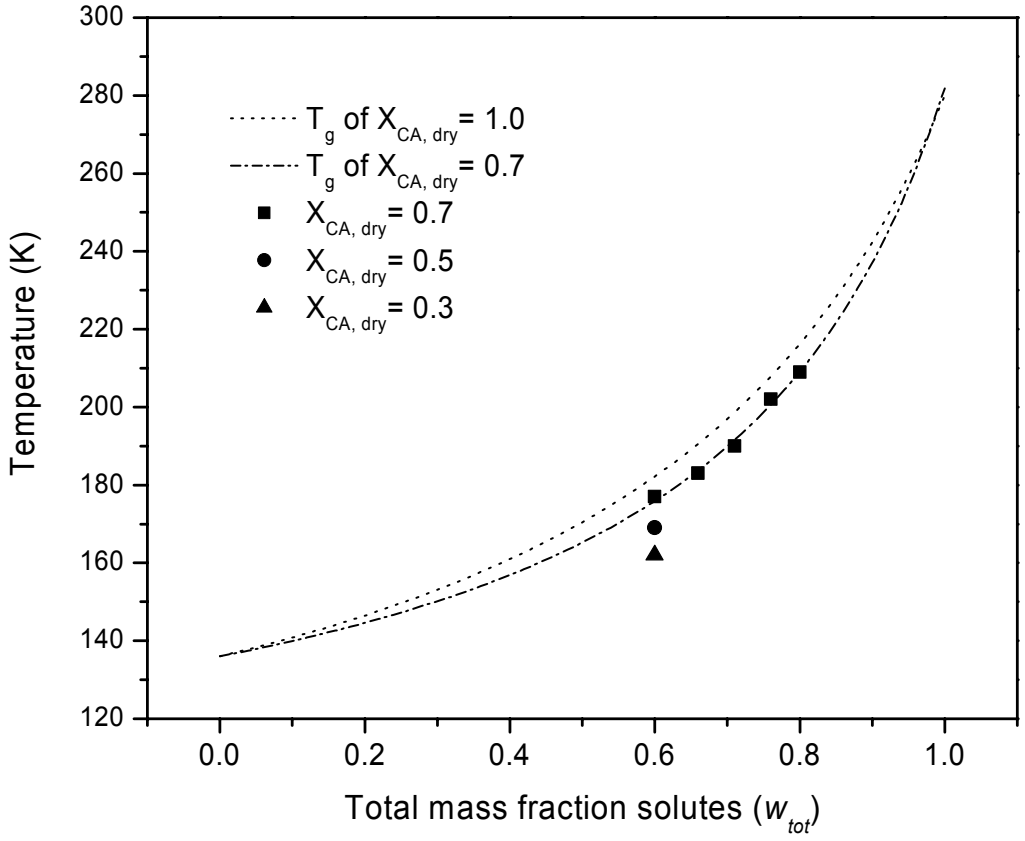


Figure 3.7: Glass transition temperatures of citric acid-ammonium sulfate solutions as a function of the total mass fraction of the solutes. Squares: $X_{CA,\ dry}$ = 0.7; circle: $X_{CA,\ dry}$ = 0.5 and triangle: $X_{CA,\ dry}$ = 0.3. The dash-dot line is a fit to the data for $X_{CA,\ dry}$ = 0.7 using equation 3.3. The dashed line is a parameterization of the glass transition temperatures of citric acid-water solutions taken from the literature (see the text for more details).

Also shown in Figure 3.7 (dashed line) is a parameterization of the glass transition temperatures of citric acid-water solutions taken from the literature[78]. The citric acid-water data correspond to $X_{CA,dry}$ =1.0.

In Figure 3.5, we have plotted the glass transition temperatures for $X_{CA,dry}$ = 1.0 and 0.7 in RH-temperature space. For both the binary and ternary system we used the e-AIM model to relate the composition of the mixtures to RH. Note, that the $T_g$-values for $X_{CA,dry}$ = 0.5 and 0.3 shown in Figure 3.7 were not included in Figure 3.5, since the e-AIM model is limited to temperatures above 180 K. The $T_g$-values for $X_{CA,dry}$ = 1.0 and 0.7

shown in Figure 3.5 should be upper limits to the $T_g$-values for $X_{CA,dry}$ = 0.0 to 0.3 (which is the composition range used in the efflorescence experiments). This is because the addition of ammonium sulfate decreases the $T_g$ of the system as shown in Figure 3.5 and Figure 3.7. As a result the $T_g$-values shown in Figure 3.5 are insufficient to argue that glass formation is responsible for the inhibition of efflorescence observed in our studies with $X_{CA,dry}$ = 0.0 to 0.3. Nevertheless it is interesting to note that the glass transition temperatures shown are very close to the temperatures and RH values where we observed inhibition of efflorescence.

### 3.3.6 Atmospheric implications

This study has shown that relatively small quantities of citric acid can completely suppress efflorescence of ammonium sulfate at low temperatures. For example, Figure 3.4 and Figure 3.5 suggest that at temperatures below 233 K, mixed citric acid-ammonium sulfate particles will not effloresce if $X_{CA,dry} \geq 0.2$. This corresponds to a dry organic component mass fraction (organic/(organic + sulfate)) of ≥ 0.33. Recent field studies using single particle mass spectrometry suggests that the dry organic component mass fraction in the upper troposphere is 0.3 to 0.8[94]. If we assume that 60% to 90% of the total organics mass is water soluble[95,96] in the free troposphere, we obtained a water soluble organics mass fraction (organic component mass/(organic component mass+sulfate mass)) of 0.18 to 0.72. It is interesting to note that the dry organic mass fraction were we see inhibition of efflorescence (≥ 0.33) is within the composition range of importance in the atmosphere (0.18 to 0.72). The current study is only a first step toward understanding the ERH properties of mixed organic-inorganic particles in the middle and upper troposphere. Additional studies are required on other model organic systems. Nevertheless our data does point out that the efflorescence properties of mixed organic-inorganic particles can be different at low temperatures compared to room temperature and only small amounts of water soluble organic material may be needed to inhibit efflorescence of ammonium sulfate. As a result, particles in the upper troposphere may be more likely to remain in the liquid state than previously thought, and solid ammonium sulfate may be less likely to participate in heterogeneous ice nucleation in the upper troposphere.

At mentioned above, we see a different trend to that observed by Wise et al.[64] who used particles composed of palmitic acid and ammonium sulfate. The palmitic acid results may be more relevant to conditions where the organics are insoluble in water. Our citric acid results may be more relevant for conditions where the organics are water soluble and do not effloresce (i.e. remain in the liquid state or glass state) for atmospheric conditions.

## 3.4 Conclusions

We studied the efflorescence properties of mixed citric acid-ammonium sulfate particles as a function of temperatures to better understand the efflorescence properties mixed organic-inorganic particles in the middle and upper troposphere. Our data for 293 K illustrate that the addition of citric acid decreases the ERH of ammonium sulfate in the particles, which is consistent with the trends observed with other highly oxygenated organic systems. At low temperatures the trend is qualitatively the same, but at these low temperatures efflorescence can be inhibited by smaller concentrations of citric acid. In other words, this study shows that at low temperatures, relatively small quantities of citric acid can completely suppress the efflorescence of ammonium sulfate. For example, at temperatures < 240 K a citric acid dry mole fraction of only 0.2 is need to inhibit efflorescence ammonium sulfate in the particles. This corresponds to a dry organic mass fraction of only 0.33. In the upper troposphere the dry mass fraction of water soluble organics is often larger than this value. Additional studies are required on other model organic systems. Nevertheless our data does point out that the efflorescence properties of mixed organic-inorganic particles can be different at low temperatures compared to room temperature and only small amounts of water soluble organic material may be needed to inhibit efflorescence of ammonium sulfate. As a result, particles in the upper troposphere may be more likely to remain in the liquid state than previously thought and solid ammonium sulfate may be less likely to participate in heterogeneous ice nucleation in the upper troposphere.

# 4 Liquid-Liquid Phase Separation and Phase Transitions of HMMA-Ammonium Sulfate Particles at Tropospheric Temperatures

## 4.1 Introduction

Aerosols are an important component of the atmosphere with effects on health, climate and atmospheric chemistry. In the atmosphere aerosols can undergo a variety of chemical and physical transformations, one such transformation is liquid-liquid separation. This phase separation involves the partitioning of an aerosol particle into a hydrophobic and a hydrophilic phase.

Liquid-liquid phase separation of organic particles has been proposed based on the results of thermodynamic modeling studies[40-42]. Liquid-liquid phase separation of organic-inorganic particles has also been observed in the laboratory, using mixtures of an inorganic salt, PEG-400 and water[39,43]. In this case an otherwise soluble organic compound separated from the aqueous phase due to salting-out effects. Salting out has been studied extensively, with applications in distillation and polymer science, however it has only recently been identified as important for aerosol interactions. Briefly, at low relative humidities (RH) the water becomes scarce, salt ions and organic molecules are forced to interact unfavourably which prompts the formation of an outer organic shell and an inner aqueous-electrolyte core.

Despite recent work, the atmospheric significance of liquid-liquid phase separation in mixed organic-inorganic particles (due to salting out effects) is still poorly understood. The effect of different inorganic components has been investigated in one study[39], but the effects of other atmospheric parameters have been largely unexamined. This study investigates the temperature dependence of liquid-liquid phase separations on mixed organic-inorganic particles at temperatures down to 233K. The effects of this separation on efflorescence and deliquescence are also investigated. Efflorescence and deliquescence are phase transitions between a crystalline and aqueous droplet which is caused by water loss or uptake, respectively. These phase transitions in mixed organic-inorganic aerosols have been studied at room temperature[34,35,58] and a small number of studies have investigated lower temperatures[64,97]. In general, studies have found that the

addition of organics tends to lower the efflorescence relative humidity (ERH) and the deliquescence relative humidity (DRH).

The phase transitions discussed above have been shown to be important to the atmosphere in several ways. Efflorescence and deliquescence influence both direct and indirect light scattering, while liquid-liquid phase separations change composition dramatically. Changes in composition influence other properties such as water uptake, organic uptake, reactivity, and mass, thus liquid-liquid separations may have a substantial effect on aerosol behaviour.

The following studies focus on aqueous mixtures of 3-hydroxy-4-methoxy mandelic acid (HMMA) and ammonium sulfate (AS). HMMA is a water-soluble, aromatic carboxylic acid and represents a partially oxidized atmospheric organic[75]. Ammonium sulfate is a very common anthropogenic inorganic aerosol component.

In the following we investigate the liquid-liquid separations observed in aqueous HMMA-ammonium sulfate solutions at temperatures from 293 K to 233 K. In solutions which phase separate we also investigate the temperature dependence of efflorescence and deliquescence. Finally, the variation observed in phase transitions with temperature is compared to known glass transition temperatures.

## 4.2 Experimental

The technique used to study phase transitions has been described in detail in literature[35,58,79] and in Chapter 3. A brief overview is provided here with a focus on details specific to the current experiments. The system consists of an optical microscope coupled to a temperature controlled flow cell. The bottom surface of the flow cell is a hydrophobic glass slide upon which the particles of interest are deposited and observed. Relative humidity in the cell was controlled by a continuous flow of a mixture of humid and dry $N_2$ (Praxair, 5.0 purity). Typical flow rates were approximately 1.5 L/min.

Phase separation and deliquescence measurements used unpolarized light, but experimental conditions were otherwise similar to previous efflorescence work. Each efflorescence and deliquescence experiment consisted of 3-15 visible particles ranging in size from 10-50 μm in diameter. Phase separations were more easily visible in larger particles, so when specifically investigating separations particles in the 30-50 μm size range were used more frequently. For each particle, the phase separation RH was

identified as the RH at which there was a clear distinction between the two phases and the efflorescence relative humidity (ERH) was identified as the RH at which the first appearance of solid was observed, even if the particles appeared only partially crystalline.

Ammonium sulfate (Fisher, 99.8%) and HMMA (Sigma-Aldrich, ≥98%) were used as supplied. Bulk mixtures were prepared gravimetrically and dissolved in Millipore filtered water (18.2 MΩ). All solutions were used within 24 hours of preparation. To prepare the particles the solution was passed through a nebulizer to produce submicron particles. These particles were directed towards a hydrophobic glass slide where they coagulated into supermicron droplets.

## 4.3 Results

The data were separated into two groups, phase transitions observed while the RH decreases from high to low and those observed as the RH increases from low to high. This separation simplifies the identification of individual trends. While examining this system it was noted that particles where $X_{HMMA,dry} \geq 0.8$ underwent no transitions, all of these particles appear liquid from RH of 90% to <1%. Additionally, no morphology change was observed in these particles.

### 4.3.1 Decreasing RH: at 293 K

Droplets with $X_{HMMA,dry} < 0.8$ underwent two distinct phase transitions at room temperature while decreasing RH: a liquid-liquid phase separation (see Figure 4.1b and c) followed by efflorescence of the aqueous ammonium sulfate fraction (see Figure 4.1d). The liquid-liquid phase separation occurs at ~77% RH and is not sensitive to the concentration of HMMA. The onset of this separation is marked by the formation of small inclusions of a second phase throughout the particle, these inclusions eventually aggregate and resolve into an outer shell and inner core (see Figure 4.1).

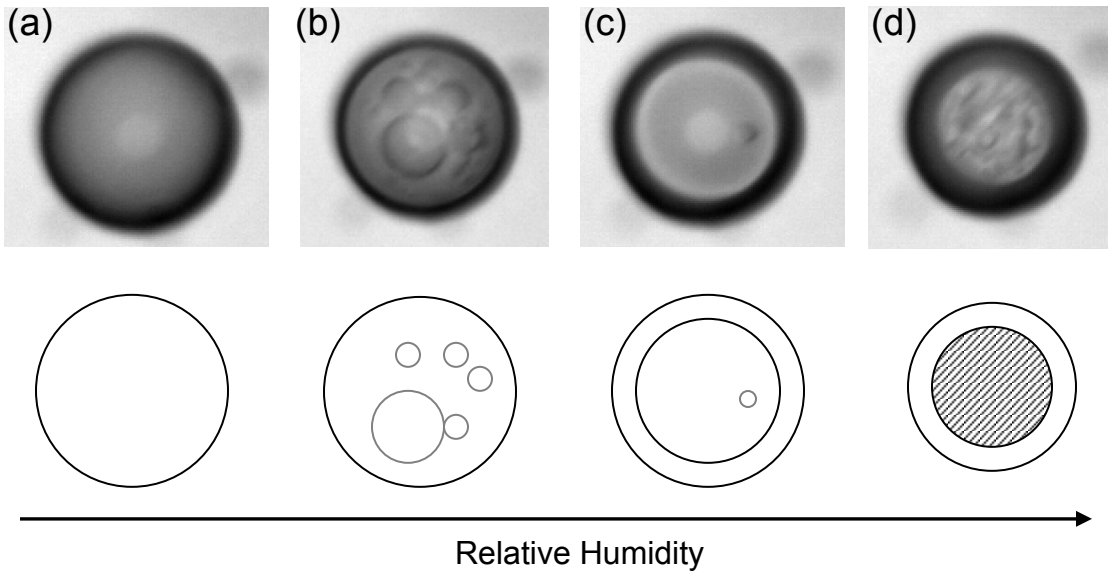


Figure 4.1: Decreasing Relative Humidity in 0.4 mol fraction HMMA. In picture (a) deliquesced particle, 85.1% RH (b) beginning of phase separation, inclusions within particle, 78.4% RH (c) phase separated particle, 75.6% RH (appearance remains constant until efflorescence) (d) inner core efflorescence, 29.2% RH

When the RH is lowered further, the inner core of the particles will effloresce at approximately 35% RH, the same range as the established ERH for pure ammonium sulfate droplets. The efflorescence is associated with a sudden change in appearance, and is illustrated in Figure 4.1. The dependence on composition of both efflorescence and phase separation is plotted in Figure 4.2. It is interesting to note that there is very little dependence on the composition. This is in direct contrast to the efflorescence suppression in particles which do not phase separate, where composition dependence has been observed in numerous studies[55,60,62,83,98-100].

It is known that the surface tension of organic compounds is lower than aqueous solutions because of the strong hydrogen bonding in aqueous water[101]. This difference in surface tension means that it is energetically more favourable for the HMMA to form the outer shell. Additionally, the inner core effloresces while the outer core does not. This is consistent with the behaviour of pure ammonium sulfate and HMMA, respectively.

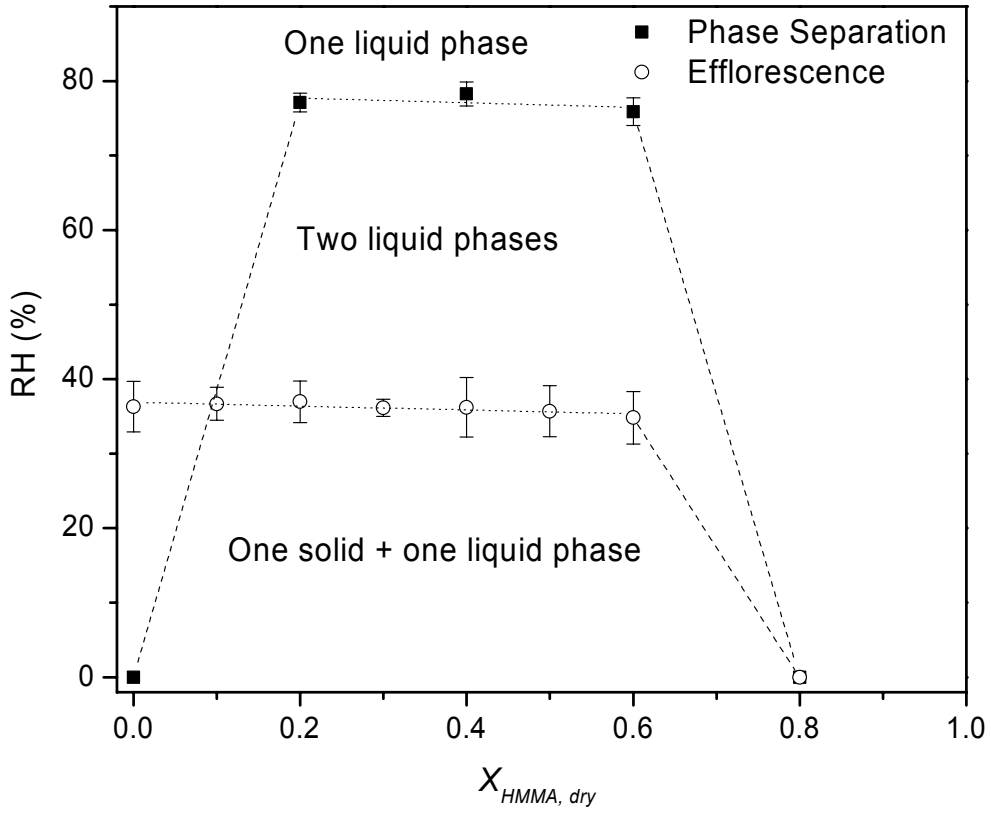


Figure 4.2: Phase diagram for HMMA-ammonium sulfate particles at room temperature and decreasing RH. The lines are to guide eye only.

### 4.3.2 Phase separation at lower temperatures

As discussed above, liquid-liquid separations were observed in all cases during room temperature measurements of particles where $X_{HMMA,dry} < 0.8$. The temperature dependence of the liquid-liquid phase separation RH is shown on Figure 4.3. Similar separations are observed at lower temperatures. For the 0.2 and 0.4 mol fractions there is a substantial overlap between the error bars, although there is some deviation from the average in the 263K case. The error bars represent a combination of $\pm 2\sigma$ (95% of cases for a normal distribution) and the instrumental uncertainties associated with the hygrometer. Mixtures typically separate at an RH of approximately 77% (within error). The measurements at 263K are statistically lower, there is no theoretical explanation for

this behaviour at this time. However, the points have been replicated and consistently yield results roughly 10% lower than the other measurements.

The behaviour when $X_{HMMA,dry}$ = 0.6 shows a more dramatic trend: at 263 K and below, the studied particles do not separate at all and appear to remain a single phase even at very low RH. It should also be noted that the phase separation at 278 K, $X_{HMMA,dry}$ = 0.6 has a different appearance and occurs at approximately 65% RH. This phase separation does not progress into a complete liquid-liquid separation and is illustrated in Figure 4.4. This change may represent a partial liquid-liquid separation which is arrested by increasing solution viscosity.

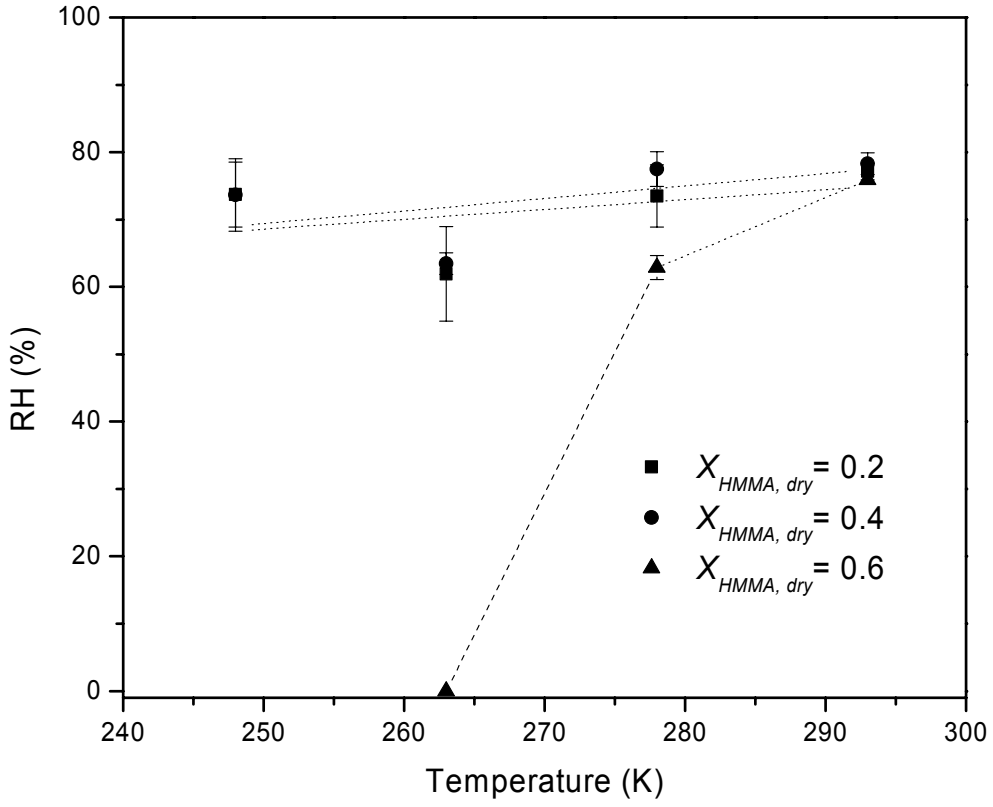


Figure 4.3: Temperature dependence of the liquid-liquid phase separation in HMMA-ammonium sulfate particles. The $X_{HMMA,dry}$ = 0.6 case ceases to phase separate at 263 K, the decrease at 278 K is discussed in greater detail in the text.

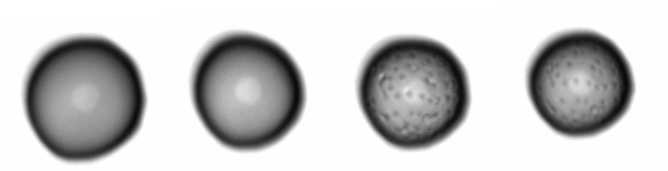

78.8% 66.6% 60.3% 48.1%

Figure 4.4: Images of $X_{HMMA,\ dry}$ = 0.6 at 278 K: the particles undergo an obvious change but do not resolve into two liquid layers. A proposed explanation for this behaviour is an increase in viscosity as the organic becomes more concentrated (see text for more details).

The inhibition of liquid-liquid phase separation when $X_{HMMA,dry}$ = 0.6 may be related to the glass transition temperature of the particles. The $T_g$ values of mixed HMMA-ammonium sulfate-water solutions are not known. However, Zobrist et al[75]. have developed a parameterization for calculating the $T_{g,mix}$ for a variety of organic-water mixtures including HMMA-water[75]. In Figure 4.5 we have plotted the glass transition temperature of a pure HMMA-water particle in equilibrium with the surrounding RH. This line corresponds to $X_{HMMA,dry}$ = 1.0, and should be considered as an upper limit to the glass transition temperatures of HMMA-ammonium sulfate-water mixtures. It is known that prior to glass formation a solution's viscosity increases dramatically (three orders of magnitude in 10°C near $T_g$)[102,103]. The increasing viscosity of the particles at $X_{HMMA,dry}$ = 0.6 is a possible explanation for the phase separation behavour under these conditions. This is not conclusive proof that glass formation or viscosity increases are impeding the separation (since the glass transitions of $X_{HMMA,dry}$ = 1.0 are only lower limits for $X_{HMMA,dry}$ = 0.6), but provides a reasonable hypothesis for further examination.

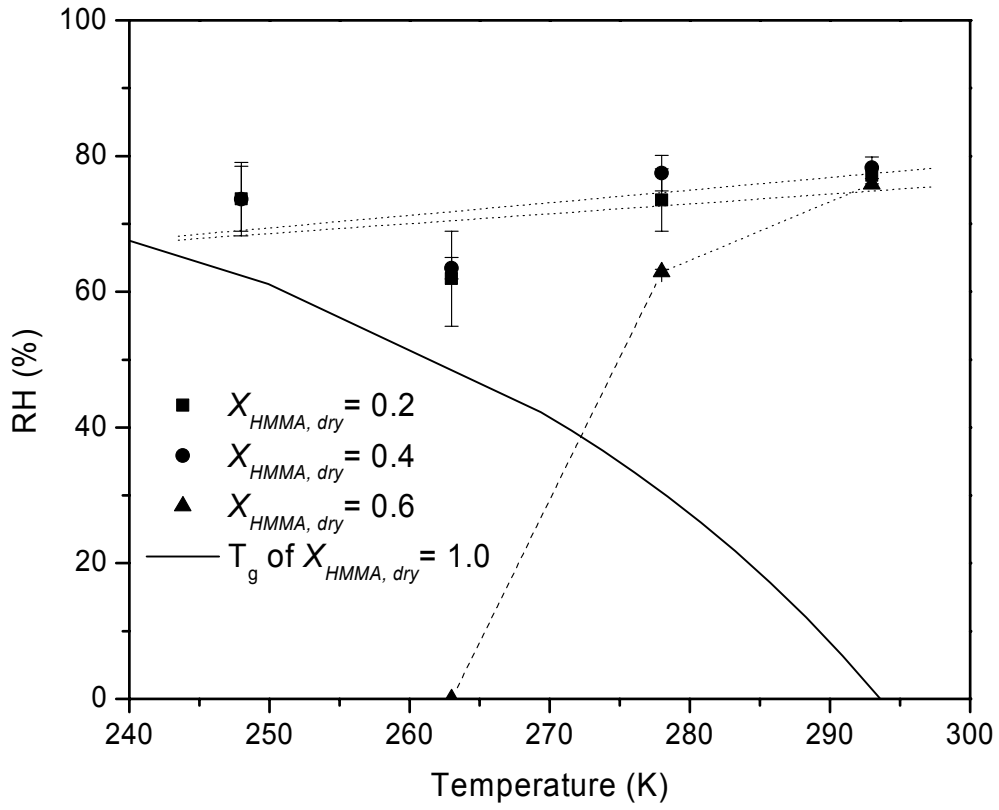


Figure 4.5: Experimental data for liquid-liquid separation and the glass transition temperature of pure HMMA-water mixture ($X_{HMMA, dry}$ = 1.0).

### 4.3.3 Efflorescence at lower temperatures

The efflorescence results and trends for this study are shown in Figure 4.6. Similar to the liquid-liquid separations results presented above, the composition $X_{HMMA,dry}$ = 0.6 shows significant temperature dependence. At 278 K these particles completely cease to effloresce, even when exposed to very low RH values (<2%). This suppression of efflorescence also applies to all compositions where $X_{HMMA,dry}$ > 0.6 which were examined at all temperatures. As discussed above, a possible explanation is that the suppression is due to formation of a glass or a viscosity increase. This glass formation would also inhibit efflorescence at lower temperatures and has been proposed to explain organic inhibition of efflorescence previously in literature[35,74,97].

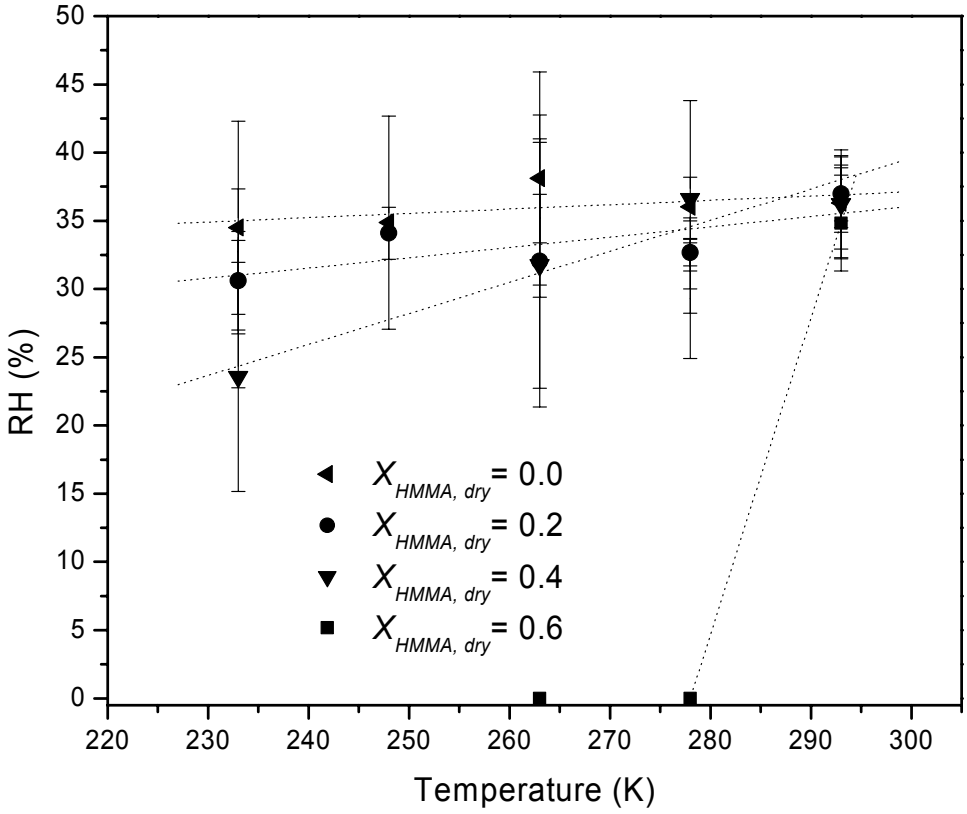


Figure 4.6: Temperature dependence of HMMA-ammonium sulfate efflorescence events. A value of 0% RH represents no observed efflorescence for a minimum of one hour.

The cases where $X_{HMMA,dry} \leq 0.4$ are somewhat different from higher concentrations. For these compositions a liquid-liquid phase separation is observed at all studied temperatures, which results in an organic coating and an aqueous inorganic-rich core. In these cases the inorganic core effloresces at approximately 35%. This is not surprising since a small amount of organic in the core is not expected to lower the ERH. However, it is surprising that the inner core maintains equilibrium with the water vapour in the cell. After liquid-liquid separation the outer shell is expected to be an HMMA-water mixture with very little inorganic material. The glass transition of pure HMMA ($X_{HMMA,dry} = 1.0$) is also shown on Figure 4.7.

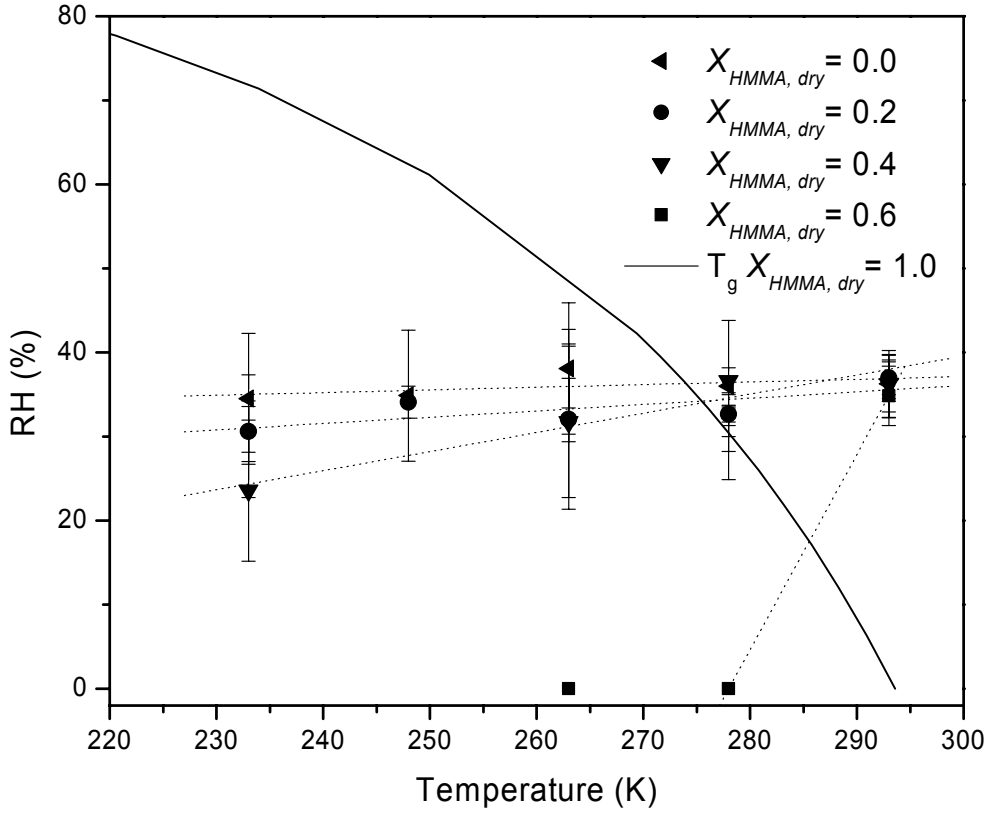


Figure 4.7: Solid line is $T_g$ of HMMA-water mixture. This shows that all measurements below 278 K are well below $T_g$, and thus outer layer should be a glass.

Figure 4.7 implies that the HMMA coating should be glassy for relevant RHs at all temperatures below 278 K. Calculations (using equations presented in Murray 2008) imply that diffusion of water through glassy HMMA should be extremely slow ~0.066 nm/min[74]. The fact that the core effloresces so close to the ERH of pure ammonuium sulfate suggests that it is in equilibrium with the surroundings, and mass transfer of water across the coating is not inhibited. We suggest two possibilities to explain this. First the HMMA outer shell may not completely surround the core. Ciobanu et al[43]. also used an experimental system where the results were a top view of μm-sized particles on a hydrophobic slide, very similar to our experimental method. By investigating contact angles they identified a range of possible particle morphologies and determined that a double spherical calotte (shown in Figure 4.8) was a likely form for 1:1 mixtures of PEG-

400 and ammonium sulfate. This morphology would be consistent with the observed results as the inner core can interact with the outside environment directly, without water vapor passing through a thick (glassy) outer shell. Similarly, Reid et al.[104,105] observed that in NaCl-decane-water systems suspended using optical tweezers, the organic only partially engulfed the aqueous fraction. These partially exposed morphologies suggest that it is atmospherically reasonable that the core may have direct exposure when suspended in the atmosphere[104,106]. As the morphology of multiphase atmospheric particles is studied further, the implications of glass transitions can be extrapolated.

Figure 4.8: Diagram of the spherical calotte morphology suggested by Ciobanu et al[43]. In this morphology the inner core is exposed to the outside environment.

Another possibility is that the coating has defects. In fact some of the images (see Figure 4.9a for example) reveal some types of defects in the coatings which may aid in mass transfer across the organic coating.

### 4.3.4 Increasing RH: room temperature

When beginning with effloresced particles that have undergone a liquid-liquid phase transition and then raising the RH, one phase transition was observed (see Figure 4.9). The effloresced inner core takes up water, shrinking and eventually deliquescing as the RH reaches 80%. This is also similar to pure ammonium sulfate. There appears to be little dependence on particle composition as shown in Figure 4.10. The images presented in Figure 4.9 are representative of the deliquescence process, it is important to note that the particles deliquesce into a single liquid phase. This behaviour differs from PEG-400-ammonium sulfate systems, which deliquesce into two liquid phases and proceed to join into a single liquid droplet at an RH near 90%[43].

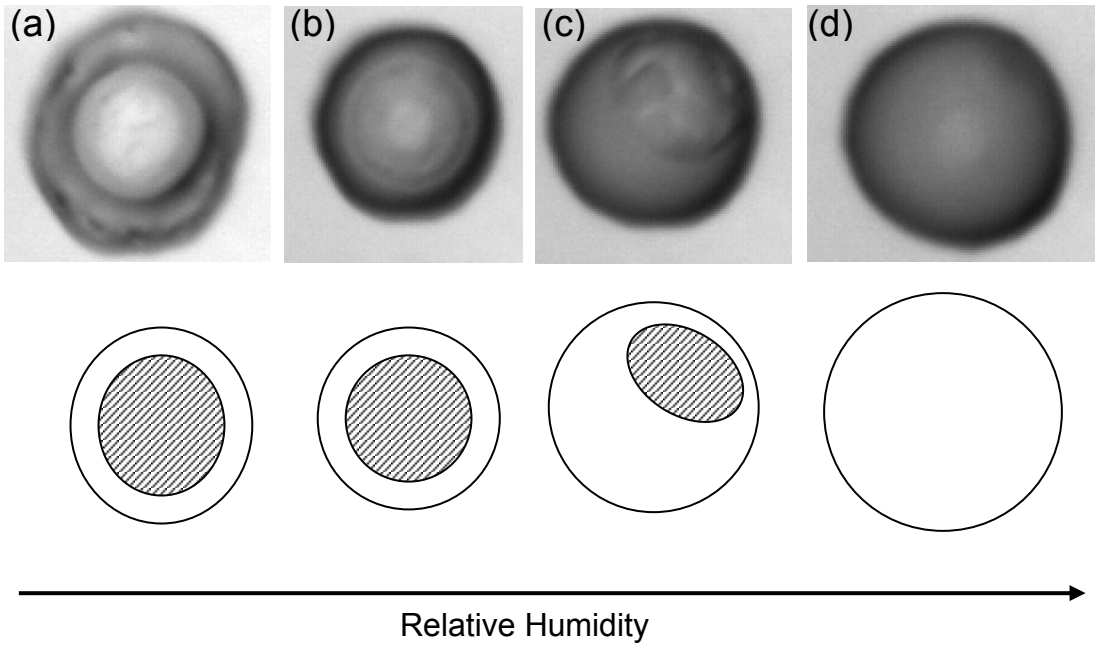


Figure 4.9: Increasing humidity in 0.4 mol fraction HMMA. Dual layer (in a and b) is caused by an outer layer of HMMA and inner effloresced core. In picture (a) effloresced core, 25.3% (b) effloresced core, 62.9% (c) partially deliquesced core, 80.2% (d) fully deliquesced particle, 81.4%

As mentioned in the introduction, studies have observed liquid-liquid separations in several solutions, primarily in bulk solutions containing ammonium sulfate mixed with polyols[39] or micron sized droplets of ammonium sulfate and PEG-400[43]. These separations occurred at 80% (AS+1,4 butadiol) and 95% (AS + 1,2 hexadiol). When considering other inorganic salts, such as ammonium nitrate, this range increases even further. The large variation between where similar compounds phase separate is different from deliquescence of mixed particles; the DRH changes less dramatically with organic addition. This suggests that the deliquescence into a single phase observed in this study and the deliquescence into two phases observed by Ciobanu et al.[43] could simply be a result of substantial variation in the phase separation, which is consistent with our observations.

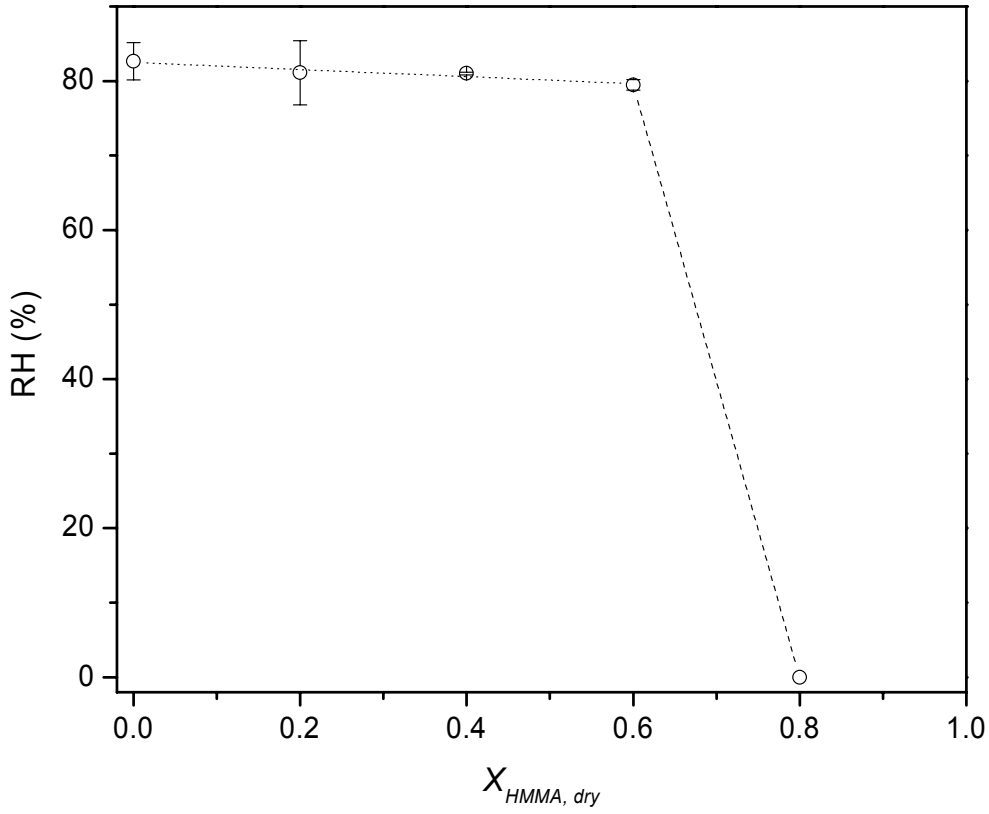


Figure 4.10: Deliquescence of HMMA-ammonium sulfate particles at room temperature with increasing RH. A value of 0% RH represents no observed efflorescence (and thus, no deliquescence).

### 4.3.5 Deliquescence at lower temperatures

Unlike the efflorescence behaviour, the temperature dependence of the deliquescence is relatively straightforward. Measurements at 233 K were found to be impossible because ice nucleated consistently; this is not surprising as $S_{ice}$ at the expected DRH is 117%. With a high supersaturation with respect to ice and many liquid droplets available, nucleation of ice is inevitable. As discussed above, particles where $X_{HMMA,dry}$ = 0.6 do not effloresce at temperatures of 263 K and below. However, it was possible to effloresce these particles at higher temperatures and then lowering the temperature to the desired value for low temperature deliquescence experiments. As shown in Figure 4.11 the error bars for all trials where $X_{HMMA,dry} \geq 0$ overlap significantly. This shows that there

is no discernable difference for different compositions and essentially no dependence on temperature for deliquescence. Comparison between pure ammonium sulfate deliquescence ($X_{HMMA,dry}$ = 0.0) and binary mixtures does show a small decrease in DRH. This decrease has been well documented in other ammonium sulfate-organic mixtures and is of a comparable amount[58,59,98,100].

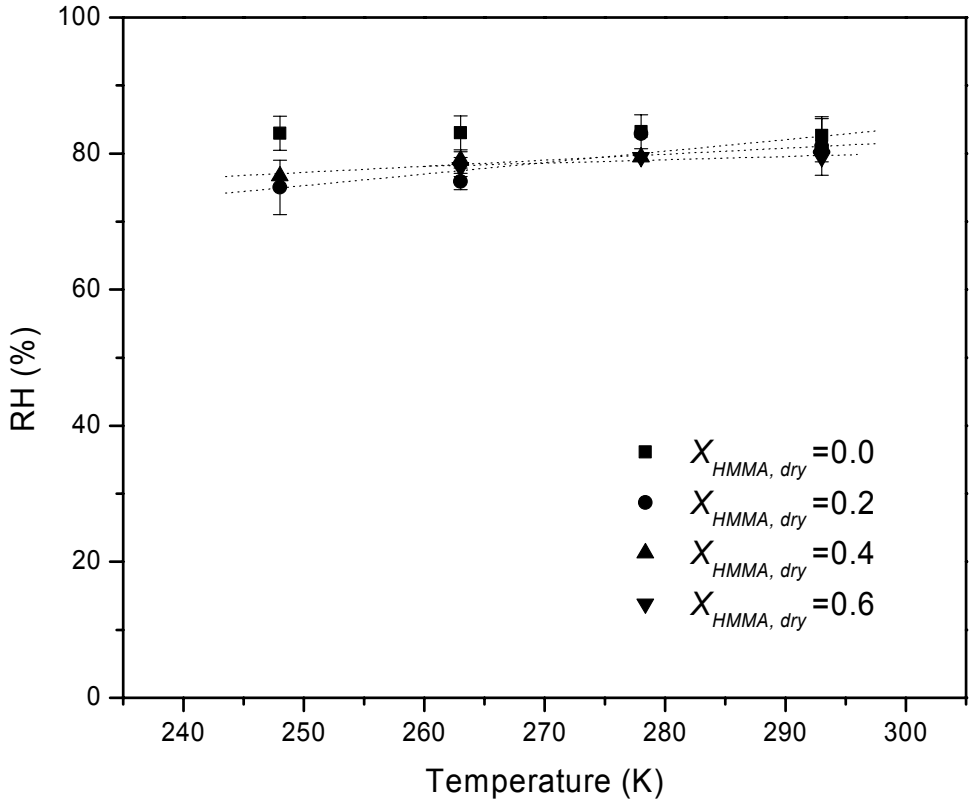


Figure 4.11: Temperature deliquescence of HMMA-ammonium sulfate particles. For low temperature measurements of $X_{HMMA,\ dry}$ = 0.6 particles, efflorescence occurred at room temperature and deliquescence occurred at the reported temperature.

## 4.4 Conclusions

A variety of phase transitions have been observed over a range of temperatures and compositions in the mixed organic-inorganic particles studied. This study provides insight into the behaviour of organic-inorganic mixtures in the atmosphere, and it is especially relevant for aromatic organics with relatively low organic to carbon (O:C)

ratios. Low temperature measurements are particularly applicable for aerosols in the upper troposphere and tropopause, where the abundance of sulfate-organic particles is high. The low temperature phase separation behaviour influences composition and thus, a wide variety of aerosol properties.

The studied particles were found to effloresce and phase separate at compositions where $X_{HMMA,dry} \leq 0.4$ at all temperatures. For particles were $X_{HMMA,dry} = 0.6$, phase separation is inhibited at 263 K and efflorescence ceases at 278 K. It is believed that the suppression of efflorescence and phase separation at lower temperatures stems from an increase in solution viscosity or formation of a glass. This hypothesis is supported by the known glass transition temperatures of water-HMMA mixtures. The continued efflorescence of liquid-liquid phase separated particles when the outer core is glassy has provided further insight into the morphology of these particles. Further studies investigating the morphology of atmospheric phase separated particles can clarify whether the inner core is only partially engulfed or whether defects in the glassy shell are responsible for this behaviour.

This study has also investigated the deliquescence behaviour of mixed inorganic-organic particles at low temperatures. These investigations are less novel, as a substantial body of work investigating deliquescence in mixed particles exists. A small decrease in ammonium sulfate's DRH was observed (a decrease of 4% at most), this consistent with behaviour according to literature.

# 5 Concluding Remarks and Future Work

## 5.1 Summary of work

This thesis has investigated the phase transition behaviour of several mixed organic-inorganic compounds. This behaviour has significant consequences in several different fields including human health, visibility, atmospheric reactivity and climate change. In order to develop a more accurate picture of the upper troposphere and tropopause the studies contained in this thesis have examined behaviour at temperatures down to 233 K and mixtures containing ammonium sulfate, the most common inorganic component in the atmosphere. The two different organics investigated throughout this work, citric acid and HMMA demonstrate markedly different behaviour in their phase separations. The key difference between the two compounds is that HMMA demonstrated liquid-liquid phase separations caused by salting out effects while citric acid mixtures never phase separate at any point during the experiments. Current work differentiating these regimes shows that O:C ratio may be a good indicator of whether an organic will promote phase separation by salting out, with high O:C ratios remaining a single phase while low ratios imply liquid-liquid phase separation as the RH decreases.

The studies investigating citric acid-ammonium sulfate mixtures demonstrated that citric acid was substantially more efficient in impeding efflorescence of ammonium sulfate at room temperature when compared to other organics. The low temperature measurements showed that smaller concentrations of citric acid were able to inhibit efflorescence at lower temperatures. The efflorescence inhibition results have been correlated with the glass transition temperatures of water-citric acid mixtures. The $T_g$ behaviour corresponds well to the efflorescence suppression, providing support for a modified model of classical nucleation theory which incorporates solution viscosity. It is important to note that the experiments described herein do not explicitly prove that viscosity increases are responsible for the efflorescence inhibition but do provide additional support for the hypothesis. This result has important consequences, it implies that previous work may overestimate the amount of solid sulfate particles in the upper atmosphere. This in turn could influence ice cloud formation, light scattering and heterogeneous atmospheric chemistry.

The HMMA-ammonium sulfate studies also demonstrated inhibition of efflorescence at lower temperatures. An additional phase separation effect was observed in this system, caused by salting out interactions between the aqueous inorganic ions and the organic component. The differences in surface tension cause the organic to form an outer shell while the aqueous inorganic components form an inner shell. The outer shell contains almost no ammonium or sulfate ions, and is expected to form a glass at atmospherically relevant RH values. The ammonium sulfate cores demonstrated similar ERH values to previous experiments, this is only possible if the core has some exposure to the external RH without interference from the glassy shell. Two possible morphologies were suggested; defects in the glassy shell or partial encapsulation of the core by the shell, the later is consistent with observations by both Ciobanu[43] (on a substrate) and theoretical predictions for immiscible systems by Reid et al[104]. The phase separation observed in this system also has important ramifications for atmospheric aerosols, the changes in composition associated with phase separation have the potential to alter reactivity, water uptake and other important aerosol properties.

As a whole, this thesis has provided new insight into the phase transitions which atmospheric particles undergo. The most novel aspect of these investigations has been a focus on the temperature dependence of these transitions in addition to investigating the effects of composition. A strong temperature dependence resulted in efflorescence inhibition in both systems and some phase separation inhibition for the $X_{HMMA,\ dry} = 0.6$ case. These results can be used to better understand the effects of atmospheric aerosols and their effects.

## 5.2 Future work and direction

There are several avenues for further study and application of the ideas broached in this thesis. Low temperature investigations of mixed particles are still rare and the results herein show that behaviour at room temperature can not necessarily be extrapolated to lower temperature analogs. Additional studies investigating different species or mixtures would be valuable to ensure that the phase behaviour of citric acid and HMMA mixtures can be generalized more broadly. Studies investigating the behaviour of real world secondary organic aerosol mixtures would be exciting for similar reasons.

Additional study of the viscosity and glass formation in atmospherically relevant aerosols is also important. Existing descriptions of glass formation are primarily semi-empirical and optimized for application in polymer or food-preparation systems. A more detailed investigation of the effects of different salts and organics, or even investigations of collected SOA samples may be able to provide proof that glass formation is directly influencing efflorescence and nucleation in atmospheric systems. A related study which is also important is investigating the ice nucleation properties of glassy particles. This subject has important consequences for determining the indirect effect of glassy particles and has just begun to be investigated[76,107].

Further investigation of the glassy, phase separated particle's morphology is also extremely important. This poses several experimental challenges, a reasonable starting point may be adaptation of the theoretical model proposed by J.P. Reid[104] to salting out systems (rather than purely immiscible ones). Although it is widely held that the hydrophobic glass slides do not influence the particle's chemistry, it would be valuable to investigate particle structure in an EDB or similar levitated system based on Ciobanu's observation of the spherical calotte morphology[43]. Finally, a long term research goal is the incorporation of these results into existing climate models. This work will require collaboration between experimental, field and modeling studies and is currently a distant project. It is important to remember that incorporation into global climate models is a key application for phase transition studies of this nature.

# References


1 Finlayson-Pitts, B. J. and J. N. Pitts (2000). Chemistry of the Upper and Lower Atmosphere: Theory, Experiments and Applications. San Diego, CA, Academic Press.

2 Whitby, K. T. and G. M. Sverdrup, Advances in Environmental Science and Technology, 1980, **8**: 477-525.

3 Pope, C. A. and D. W. Dockery, J. Air Waste Manage. Assoc., 2006, **56**(6): 709-742.

4 Wallace, J. M. and P. V. Hobbs (2006). Atmospheric Science: an introductory survey, Elsevier Inc.

5 Slinn, W. G. N., Atmos. Environ., 1975, **9**(8): 763-764.

6 Ellison, G. B., A. F. Tuck and V. Vaida, J Geophys Res-Atmos, 1999, **104**(D9): 11633-11641.

7 Gelencser, A. (2004). Carbonaceous Aerosol. Dordrecht, The Netherlands, Springer.

8 Kroll, J. H. and J. H. Seinfeld, Atmos. Environ., 2008, **42**(16): 3593-3624.

9 Zhang, Q., J. L. Jimenez, M. R. Canagaratna, J. D. Allan, H. Coe, I. Ulbrich, M. R. Alfarra, A. Takami, A. M. Middlebrook, Y. L. Sun, K. Dzepina, E. Dunlea, K. Docherty, P. F. DeCarlo, D. Salcedo, T. Onasch, J. T. Jayne, T. Miyoshi, A. Shimono, S. Hatakeyama, N. Takegawa, Y. Kondo, J. Schneider, F. Drewnick, S. Borrmann, S. Weimer, K. Demerjian, P. Williams, K. Bower, R. Bahreini, L. Cottrell, R. J. Griffin, J. Rautiainen, J. Y. Sun, Y. M. Zhang and D. R. Worsnop, Geophys. Res. Lett., 2007, **34**(13).

10 Kanakidou, M., J. H. Seinfeld, S. N. Pandis, I. Barnes, F. J. Dentener, M. C. Facchini, R. Van Dingenen, B. Ervens, A. Nenes, C. J. Nielsen, E. Swietlicki, J. P. Putaud, Y. Balkanski, S. Fuzzi, J. Horth, G. K. Moortgat, R. Winterhalter, C. E. L. Myhre, K. Tsigaridis, E. Vignati, E. G. Stephanou and J. Wilson, Atmos. Chem. Phys., 2005, **5**: 1053-1123.

11 Saxena, P. and L. M. Hildemann, J. Atmos. Chem., 1996, **24**(1): 57-109.

12 Murphy, D. M., D. J. Cziczo, K. D. Froyd, P. K. Hudson, B. M. Matthew, A. M. Middlebrook, R. E. Peltier, A. Sullivan, D. S. Thomson and R. J. Weber, J Geophys Res-Atmos, 2006, **111**(D23).

13 Lin, C., M. Baker and R. J. Charlson, Appl. Optics, 1973, **12**(6): 1356-1363.

14 Prather, K. A., C. D. Hatch and V. H. Grassian, Annu. Rev. Anal. Chem., 2008, **1**: 485-514.

15 Bond, T. C., G. Habib and R. W. Bergstrom, J Geophys Res-Atmos, 2006, **111**(D20).

16 Murphy, D. M., D. S. Thomson and T. M. J. Mahoney, Science, 1998, **282**(5394): 1664-1669.

17 Carmichael, G. R., B. Adhikary, S. Kulkarni, A. D'Allura, Y. H. Tang, D. Streets, Q. Zhang, T. C. Bond, V. Ramanathan, A. Jamroensan and P. Marrapu, Environ. Sci. Technol., 2009, **43**(15): 5811-5817.

18 Thornton, J. A., C. F. Braban and J. P. D. Abbatt, Phys. Chem. Chem. Phys., 2003, **5**(20): 4593-4603.

19 Hallquist, M., D. J. Stewart, S. K. Stephenson and R. A. Cox, Phys. Chem. Chem. Phys., 2003, **5**(16): 3453-3463.

20 Wark, K., C. F. Warner and W. T. Davis (1998). Air Pollution: its origin and control. Menlo Park, California, Addison Wesley Longman, inc.

21 Solomon, S. D., M. Qin, Z. Manning, M. Chen, K. B. Marquis, M. Averyt and T. a. H. L. M. (eds.), Eds. (2007). IPCC, 2007: Climage Change 2007: The Physical Science Basis. Contribution of Working Group I to the Fourth Assessment Report of the Intergovernmental Panel on Climate Change. Cambridge, U.K. and New York, NY, USA, Cambridge University Press.

22 Tie, X., D. Wu and G. Brasseur, Atmos. Environ., 2009, **43**(14): 2375-2377.

23 Cho, Y. S., J. T. Lee, C. H. Jung, Y. S. Chun and Y. S. Kim, J. Environ. Health, 2008, **71**(2): 37-43.

24 Clegg, S. L., J. H. Seinfeld and P. Brimblecombe, Journal of Aerosol Science, 2001, **32**(6): 713-738.

25 Clegg, S. L. and J. H. Seinfeld, J Phys Chem A, 2006, **110**(17): 5692-5717.

26 Clegg, S. L. and J. H. Seinfeld, J Phys Chem A, 2006, **110**(17): 5718-5734.

27 Clegg, S. L., P. Brimblecombe and A. S. Wexler (e-AIM). Extended AIM Aerosol Thermodynamics Model, http://www.aim.env.uea.ac.uk/aim/aim.php.

28 Mullin, J. W. (2001). Crystallization, Elsevier Ltd.

29 Papon, P., J. Leblond and P. H. E. Meijer (2002). The Physics of Phase Transitions: Concepts and Applications. Berlin,Heidelberg, New York, Springer-Verlag.

30 Pruppacher, H. R. and J. D. Klett (1998). Microphysics of Clouds and Precipitations. Dordrecht, The Netherlands, Kluwer Academic Publishers.

31 Volmer, M. (1939). Kinetic der Phasenbildung. Leipzig, Steinkopff.

32 Gibbs, J. W. (1948). collected works. New Haven, Yale University Press.

33 Becker, R. and W. Dorring, Annalen der Physik, 1935, **24**: 719-752.

34 Parsons, M. T., J. L. Riffell and A. K. Bertram, J Phys Chem A, 2006, **110**(26): 8108-8115.

35 Parsons, M. T., D. A. Knopf and A. K. Bertram, J Phys Chem A, 2004, **108**(52): 11600-11608.

36 Tang, I. N. and H. R. Munkelwitz, Atmospheric Environment Part a-General Topics, 1993, **27**(4): 467-473.

37 Seinfeld, J. H. and S. N. Pandis (1998). Atmospheric Chemistry and Physics: From Air Pollution to Climate Change. New York, Wiley.

38 Cruz, C. N. and S. N. Pandis, Environ. Sci. Technol., 2000, **34**(20): 4313-4319.

39 Marcolli, C. and U. K. Krieger, J Phys Chem A, 2006, **110**(5): 1881-1893.

40 Pun, B. K., R. J. Griffin, C. Seigneur and J. H. Seinfeld, J Geophys Res-Atmos, 2002, **107**(D17).

41 Griffin, R. J., K. Nguyen, D. Dabdub and J. H. Seinfeld, J. Atmos. Chem., 2003, **44**(2): 171-190.

42 Erdakos, G. B. and J. F. Pankow, Atmos. Environ., 2004, **38**(7): 1005-1013.

43 Ciobanu, V. G., C. Marcolli, U. K. Krieger, U. Weers and T. Peter, J Phys Chem A, 2009, **113**(41): 10966-10978.

44 Furter, W. F., Can. J. Chem. Eng., 1977, **55**(3): 229-239.

45 Furter, W. F. and R. A. Cook, Int. J. Heat Mass Transf., 1967, **10**(1): 23-&.

46 Long, F. A. and W. F. McDevit, Chem. Rev., 1952, **51**(1): 119-169.

47 Buzorius, G., A. Zelenyuk, F. Brechtel and D. Imre, Geophys. Res. Lett., 2002, **29**(20).

48 Marcolli, C., B. P. Luo and T. Peter, J Phys Chem A, 2004, **108**(12): 2216-2224.

49 Martin, S. T., H. M. Hung, R. J. Park, D. J. Jacob, R. J. D. Spurr, K. V. Chance and M. Chin, Atmos. Chem. Phys., 2004, **4**: 183-214.

50 Wang, J., A. A. Hoffmann, R. J. Park, D. J. Jacob and S. T. Martin, J Geophys Res-Atmos, 2008, **113**(D11).

51 Alshawa, A., O. Dopfer, C. W. Harmon, S. A. Nizkorodov and J. S. Underwood, J Phys Chem A, 2009, **113**(26): 7678-7686.

52 Zelenyuk, A., D. Imre, L. A. Cuadra-Rodriguez and B. Ellison, Journal of Aerosol Science, 2007, **38**(9): 903-923.

53 Woods, E., H. S. Kim, C. N. Wivagg, S. J. Dotson, K. E. Broekhuizen and E. F. Frohardt, J Phys Chem A, 2007, **111**(43): 11013-11020.

54 Lightstone, J. M., T. B. Onasch, D. Imre and S. Oatis, J Phys Chem A, 2000, **104**(41): 9337-9346.

55 Brooks, S. D., R. M. Garland, M. E. Wise, A. J. Prenni, M. Cushing, E. Hewitt and M. A. Tolbert, J Geophys Res-Atmos, 2003, **108**(D15).

56 Braban, C. F. and J. P. D. Abbatt, Atmos. Chem. Phys., 2004, **4**: 1451-1459.

57 Choi, M. Y. and C. K. Chan, Environ. Sci. Technol., 2002, **36**(11): 2422-2428.

58 Pant, A., A. Fok, M. T. Parsons, J. Mak and A. K. Bertram, Geophys. Res. Lett., 2004, **31**.

59 Zardini, A. A., S. Sjogren, C. Marcolli, U. K. Krieger, M. Gysel, E. Weingartner, U. Baltensperger and T. Peter, Atmos. Chem. Phys., 2008, **8**(18): 5589-5601.

60 Yeung, M. C., A. K. Y. Lee and C. K. Chan, Aerosol Sci. Technol., 2009, **43**(5): 387-399.

61 Takahama, S., R. K. Pathak and S. N. Pandis, Environ. Sci. Technol., 2007, **41**(7): 2289-2295.

62 Brooks, S. D., P. J. DeMott and S. M. Kreidenweis, Atmos. Environ., 2004, **38**(13): 1859-1868.

63 Badger, C. L., I. George, P. T. Griffiths, C. F. Braban, R. A. Cox and J. P. D. Abbatt, Atmos. Chem. Phys., 2006, **6**: 755-768.

64 Wise, M. E., K. J. Baustian and M. A. Tolbert, Proceedings of the National Academy of Sciences, 2010, **107**(15): 6693-6698.

65 Zuberi, B., A. K. Bertram, T. Koop, L. T. Molina and M. J. Molina, J Phys Chem A, 2001, **105**(26): 6458-6464.

66 Shilling, J. E., T. J. Fortin and M. A. Tolbert, J Geophys Res-Atmos, 2006, **111**(D12).

67 Abbatt, J. P. D., S. Benz, D. J. Cziczo, Z. Kanji, U. Lohmann and O. Mohler, Science, 2006, **313**(5794): 1770-1773.

68 Wise, M. E., R. M. Garland and M. A. Tolbert, J Geophys Res-Atmos, 2004, **109**(D19).

69 Wise, M. E., K. J. Baustian and M. A. Tolbert, Atmos. Chem. Phys., 2009, **9**(5): 1639-1646.

70 Jensen, E. J., L. Pfister, T.-P. Bui, P. Lawson and D. Baumgardner (2010). Ice nucleation and cloud microphysical properties in tropical tropopause layer cirrus. Atmospheric Chemistry and Physics. **10:** 1369-1384.

71 Froyd, K. D., D. M. Murphy, P. Lawson, D. Baumgardner and R. L. Herman, Atmos. Chem. Phys., 2010, **10**(1): 209-218.

72 Mullin, J. W. and C. L. Leci, Journal of Crystal Growth, 1969, **5**(1): 75-76.

73 Mullin, J. W. and C. L. Leci, Philosophical Magazine, 1969, **19**(161): 1075-&.

74 Murray, B. J., Atmos. Chem. Phys., 2008, **8**(17): 5423-5433.

75 Zobrist, B., C. Marcolli, D. A. Pedernera and T. Koop, Atmos. Chem. Phys., 2008, **8**(17): 5221-5244.

76 Murray, B. J., T. W. Wilson, S. Dobbie, Z. Cui, S. M. R. K. Al-Jumur, O. Mohler, M. Schnaiter, R. Wagner, S. Benz, M. Niemand, H. Saathoff, V. Ebert, S. Wagner and B. Karcher, 2010, **3**(4): 233-237.

77 Maltini, E., M. Anese and I. Shtylla, Cryo-Lett., 1997, **18**(5): 263-268.

78 Leinhard, D., B. Zobrist, U. K. Krieger and T. Peter, TBD, in preperation.

79 Pant, A., M. T. Parsons and A. K. Bertram, J Phys Chem A, 2006, **110**(28): 8701-8709.

80 Colberg, C. A., U. K. Krieger and T. Peter, J Phys Chem A, 2004, **108**(14): 2700-2709.

81 Cziczo, D. J. and J. P. D. Abbatt, J Geophys Res-Atmos, 1999, **104**(D11): 13781-13790.

82 Onasch, T. B., R. L. Siefert, S. D. Brooks, A. J. Prenni, B. Murray, M. A. Wilson and M. A. Tolbert, J. Geophys. Res., 1999, **104**.

83 Parsons, M. T., J. Mak, S. R. Lipetz and A. K. Bertram, J Geophys Res-Atmos, 2004, **109**(D6): art. no. D06212.

84 Koop, T., A. Kapilashrami, L. T. Molina and M. J. Molina, J Geophys Res-Atmos, 2000, **105**(D21): 26393-26402.

85 Tang, I. N., H. R. Munkelwitz and J. G. Davis, Journal of Aerosol Science, 1978, **9**(6): 505-511.

86 Spann, J. F. and C. B. Richardson, Atmos. Environ., 1985, **19**(5): 819-825.

87 Han, J. H. and S. T. Martin, J Geophys Res-Atmos, 1999, **104**(D3): 3543-3553.

88 Cziczo, D. J., J. B. Nowak, J. H. Hu and J. P. D. Abbatt, J Geophys Res-Atmos, 1997, **102**(D15): 18843-18850.

89 Tong, C. H., S. L. Clegg and J. H. Seinfeld, Atmos. Environ., 2008, **42**(21): 5459-5482.

90 Peng, C., M. N. Chan and C. K. Chan, Environ. Sci. Technol., 2001, **35**(22): 4495-4501.

91 Gordon, M. and J. S. Taylor, Journal of Applied Chemistry, 1952, **2**(9): 493-500.

92 Kohl, I., L. Bachmann, A. Hallbrucker, E. Mayer and T. Loerting, Phys. Chem. Chem. Phys., 2005, **7**(17): 3210-3220.

93 Johari, G. P., A. Hallbrucker and E. Mayer, Nature, 1987, **330**(6148): 552-553.

94 Froyd, K. D., D. M. Murphy, T. J. Sanford, D. S. Thomson, J. C. Wilson, L. Pfister and L. Lait, Atmos. Chem. Phys., 2009, **9**(13): 4363-4385.

95 Maria, S. F., L. M. Russell, B. J. Turpin and R. J. Porcja, Atmos. Environ., 2002, **36**(33): 5185-5196.

96 Krivacsy, Z., A. Gelencser, G. Kiss, E. Meszaros, A. Molnar, A. Hoffer, T. Meszaros, Z. Sarvari, D. Temesi, B. Varga, U. Baltensperger, S. Nyeki and E. Weingartner, J. Atmos. Chem., 2001, **39**(3): 235-259.

97 Bodsworth, A., B. Zobrist and A. K. Bertram, Phys. Chem. Chem. Phys., Submitted March 2010, **Submitted March 2010**.

98 Yeung, M. C., T. Y. Ling and C. K. Chan, J Phys Chem A, 2010, **114**(2): 898-903.

99 Brooks, S. D., M. E. Wise, M. Cushing and M. A. Tolbert, Geophys. Res. Lett., 2002, **29**(19).

100 Prenni, A. J., P. J. De Mott and S. M. Kreidenweis, Atmos. Environ., 2003, **37**(30): 4243-4251.

101 Shaw, D. J. (2000). Introduction to Colloid & Surface Chemistry, 4th edition, Reed Educational and Professional Publishing Ltd.

102 Angell, C. A., Chem. Rev., 2002, **102**(8): 2627-2649.

103 Debenedetti, P. G. (1996). Metastable Liquids: concepts and principles. Princeton, New Jersey, Princeton University Press.

104 Kwamena, N. O. A., J. Buajarern and J. P. Reid, J Phys Chem A, 2010, **114**(18): 5787-5795.

105 Buajarern, J., L. Mitchem and J. P. Reid, J Phys Chem A, 2007, **111**(37): 9054-9061.

106 Takahama, S., S. Liu and L. M. Russell, J Geophys Res-Atmos, **115**.

107 Murray, B. J. and E. J. Jensen, J. Atmos. Sol.-Terr. Phys., 2010, **72**(1): 51-61.